Development and Validation of the Next Generation Gyro-Landau-fluid Transport Model (TGLF)

J. Kinsey

in collaboration with
G. Staebler, R. Waltz
General Atomics

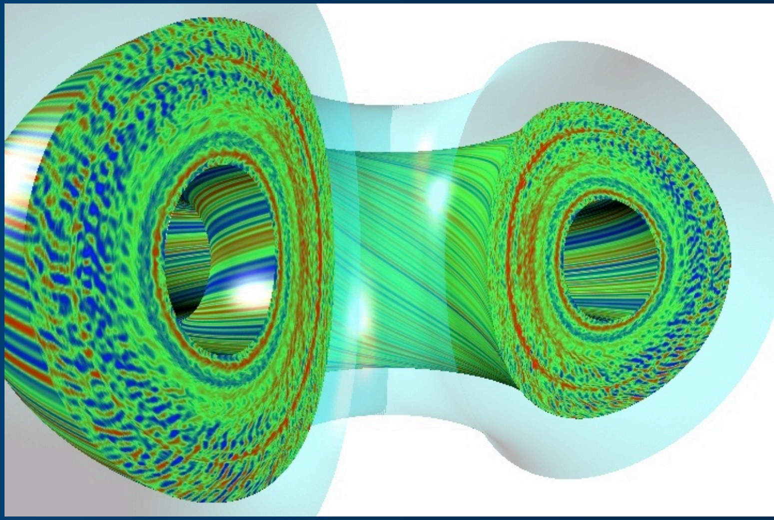

21st Transport Task Force Workshop

Mar. 25 -28, 2008
Boulder, CO

GENERAL ATOMICS

Overview

- **Philosophy in developing the Trapped Gyro-Landau-Fluid (TGLF) transport model has been to obtain best fit to gyrokinetic simulations, then use experimental data to test the theory**
- **Linear benchmarking of TGLF with GKS growth rate database**
- **Fitting of TGLF saturation rule to a nonlinear database of 83 GYRO ITG/TEM gyrokinetic simulations with shaped geometry**
  - QL theory works amazingly well ! TGLF energy fluxes within 20% of GYRO results
  - TGLF shows better agreement with GYRO simulations compared to GLF23 model and reproduces GYRO result of elongation effects on transport, ExB shear
- **Testing of TGLF transport model against experimental profile database (over 500 transport runs have been performed)**
  - Better fit to theory results in TGLF having better agreement than GLF23 with a database of 96 shots from DIII-D, JET, TFTR
- **Sensitivity Studies**
  - Boundary conditions, geometry, ExB shear
  - High-k transport
  - Finite beta effects, density evolution, boundary location
- **Summary and future work**

The TGLF Gyro-Landau-Fluid transport model

- **TGLF is the next generation GLF model with improved comprehensive physics compared to its predecessor, GLF23**
  - Model valid continuously from low-k ITG/TEM to high-k ETG
  - Extended range of validity (e.g. pedestal parameters, low aspect ratio)
  - Valid for finite aspect ratio shaped geometry using Miller local equilibrium which replaces s-α high aspect ratio shifted circular geometry
  - Includes finite beta physics, improved electron physics
- **TGLF solves for the eigenvalues using a set of 15-moment gyro-fluid equations per species for linear drift-wave instabilities using 4 Hermite basis functions (2 species x 15 eqns x 4 basis functions => 120x120 matrix)**
  - GLF23 4-moment, 2 species, 1 poloidal trial basis function => 8x8 matrix
- **For Miller model, nine parameters are required to describe the local equilibrium [1]: κ (elongation), δ (triangularity), q, s (magnetic shear), α (normalized ∇P) , $A=R_0/r$, $\partial_r R_0$, and gradient factors of κ and δ (s_κ and s_δ)**
- **TGLF has been systematically verified against a large database of linear growth rates and frequencies created using the GKS gyrokinetic code**
- **A model for the nonlinear saturation levels of the turbulence using the linear mode growth rates has been found for shaped geometry**

TGLF is a major upgrade from GLF23

TGLF

- TIM, ITG,TEM, ETG modes from a single set of equations
- Exact FLR integrals keep accuracy for high-k i.e. $k_\theta \rho_i > 1$
- Adaptive Hermite basis function solution method valid for the same range as the GK equations
- All trapped fractions
- Shaped geometry (Miller model)
- Fully electromagnetic
- New electron-ion collision model fit to pitch angle scattering
- Transport model fit to 83 GYRO runs with kinetic electrons
- 15 moment equations per species
- ≈200 times slower than GLF23

GLF23

- Different equations for low-k (ITG,TEM) and high-k (ETG)
- FLR integrals used Pade approximation valid for low-k
- Parameterized single Gaussian trial wavefunction valid for a limited range of conditions
- Small trapped fraction required.
- Shifted circle (s-α) geometry
- Normally run electrostatic
- Inaccurate electron-ion collision model only for low-k equations
- Transport model fit to a few GLF non-linear turbulence runs
- 4 moment equations per species
- Fast enough for 1997 computers!

Verification of TGLF linear growth rates using GKS gyrokinetic stability analyses

TGLF linear growth rates verified against GKS gyrokinetic stability code for 3 reference cases

- TGLF compared to GKS for numerous scans performed around 3 cases
  - 1799 linear simulations w/ kinetic electrons, s-α geometry, electrostatic
  - Scans in $k_\theta \rho_s$, q, s, a/L_T, a/L_n , r/a, Ti/Te
  - See Staebler, Kinsey, Waltz, Phys Plasmas 12, 102508 (2005)

- STD Case: Same parameters used to develop GLF23 transport model in 1996-97

R/a=3	q=2
r/a=0.5	s=1
a/L_T=3	α=0 and β=0
a/L_n=1	T_i/T_e=1

- NCS Case

  STD Case + a/L_{Ti}=10, a/L_{Te}=4, s=-0.5

- PED Case

  STD Case + r/a=0.75, a/L_T=10, a/L_n=3, q=4, s=3, α=5

TGLF demonstrated an excellent fit to the GKS linear gyrokinetic database with uniform agreement

- **Model tested around 3 reference cases:**
  - STD case: R/a=3, r/a=0.5, q=2, s=1, a/L_T=3, a/L_n=1, T_i/T_e=1, α=0 and β=0
  - PED case: STD Case + r/a=0.75, a/L_T=10, a/L_n=3, q=4, s=3, α=5
  - NCS case: STD Case + a/L_{Ti}=10, a/L_{Te}=4, s=-0.5

Avg σ_γ (STD) = 0.13 (TGLF), 0.21 (ori GLF23)

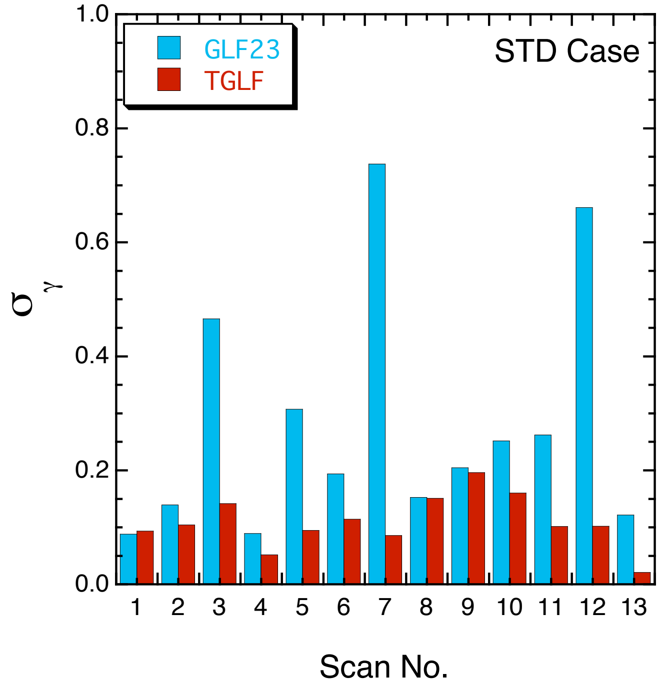

Avg σ_γ (PED) = 0.14 (TGLF), 0.54 (ori GLF23)

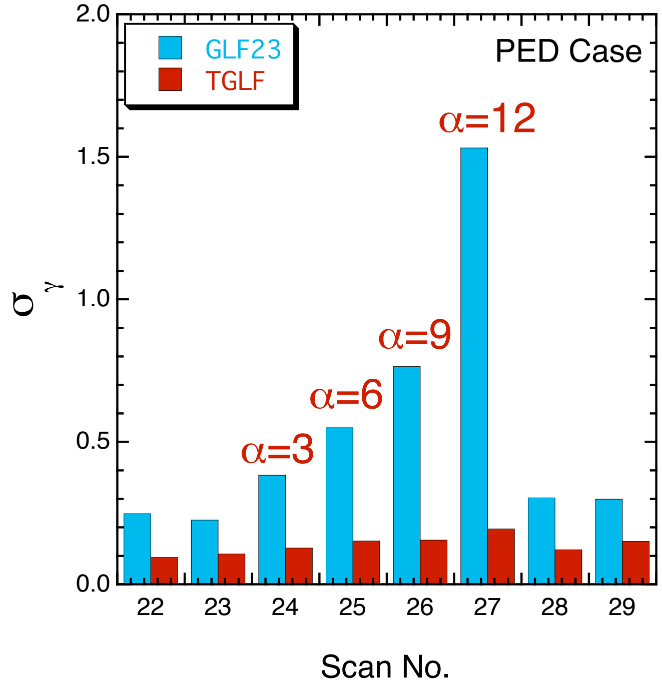

$\sigma_x=[\sum_i (X_i^{GKS}-X_i^{TGLF})^2 / \sum_i (X_i^{GKS})^2]^{1/2}$ **where X = γ or ω**

TGLF shows good agreement with GKS growth rates for DIII-D ITB discharge including real geometry, collisions

- **TGLF compared to GKS for DIII-D ITB discharges #84736**
- **The radial profile of the normalized linear growth rate for k_y = 0.3 and three different physics settings is shown**
  - (A) comprehensive physics
  - (B) collisionless, electrostatic
  - (C) s-α geometry dillution, collisionless, electrostatic
- **Reduction in growth rates w/ full physics (A) due to finite β in the inner plasma and collisions in the outer plasma**

DIII-D NCS discharge 84736 at 1.3s

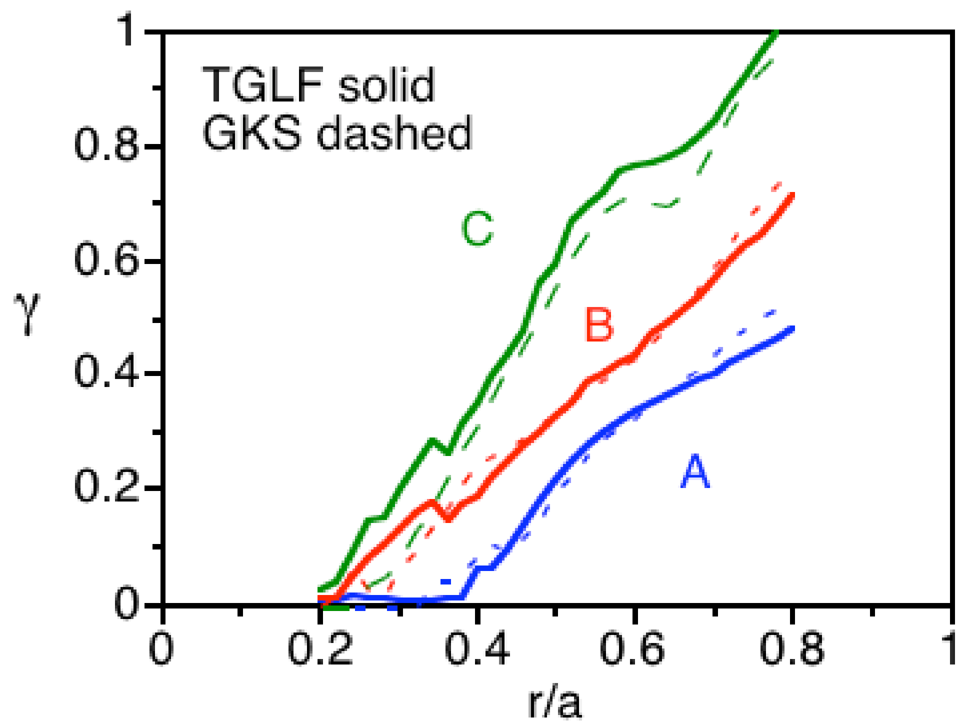

Fitting of TGLF saturation rule to nonlinear GYRO simulations

TGLF saturation rule was fit to GYRO nonlinear ITG/TEM simulations using Miller geometry

- **Transport fluxes are computed using a saturation rule with the magnitude of the total eigenvector**

$$\Gamma = \sum_{k_y} nc_s \left[\frac{\mathrm{Re}\langle i\hat{k}_y \tilde{\Phi}^* \tilde{n} \rangle}{\tilde{V}^* \tilde{V}} \right] \overline{V}^2 \quad Q = \frac{3}{2} \sum_{k_y} pc_s \left[\frac{\mathrm{Re}\langle i\hat{k}_y \tilde{\Phi}^* \tilde{p}_T \rangle}{\tilde{V}^* \tilde{V}} \right] \overline{V}^2$$

[ ] = quasilinear weight

$$\overline{V}^2 = C_{norm} \left(\frac{\rho_s \hat{\omega}_{d0}}{a} \right)^2 \left(1 + \frac{T_e}{T_i} \right)^2 \left(\frac{1}{\hat{k}_y^{c_k}} \right) \left[\frac{\hat{\gamma}_{net}^{c_1} + c_2 \hat{\gamma}_{net}}{\hat{k}_y^4} \right]$$

Model for saturated intensity

$$C_{norm} = 32.5 \quad c_1 = 1.55 \quad c_2 = 0.534 \quad \alpha_E = 0.3\sqrt{\kappa} \quad 0.1 \le \hat{k}_y \le 24$$ (21 modes)

$$\tilde{V} = (\tilde{n}, \tilde{u}_{\|}, \tilde{p}_{\|}, \tilde{p}_T, \tilde{q}_{\|}, \tilde{q}_T) \quad \hat{\gamma}_{net} = Max\left[(\hat{\gamma} - \alpha_E \hat{\gamma}_E)/\hat{\omega}_{d0}, 0 \right] \quad \hat{\omega}_{d0} = \hat{k}_y \frac{a}{R}$$

- **Coefficients & exponents in the saturation rule are found by minimizing the error between TGLF & GYRO energy fluxes for 83 nonlinear GYRO ITG/TEM simulations**

$$c_k = 0.0 \quad for \quad \hat{k}_y < 1$$

- **The high-k ($\hat{k}_y$ > 1) part of the electron energy flux is adjusted to fit one GYRO coupled ITG/TEM-ETG simulation of the GA STD case with Miller geometry by modifying the k_y exponent**

$$c_k = 1.25 \quad for \quad k_y \ge 1$$

TGLF saturation rule fits the energy transport from 83 nonlinear GYRO Miller geometry simulations very well

- **GYRO scans : kinetic electrons, Miller geometry, electrostatic, collisionless**
  - Also a version of TGLF fit to 86 shifted circle GYRO simulations
- **Use the 2 most unstable modes at each k_y**
- **Best fit has RMS errors of [17%, 20%] for [ion, electron] energy fluxes**

$\sigma_Q = [\sum_i (Q_i^{GYRO} - Q_i^{TGLF})^2 / \sum_i (Q_i^{GYRO})^2]^{1/2}$

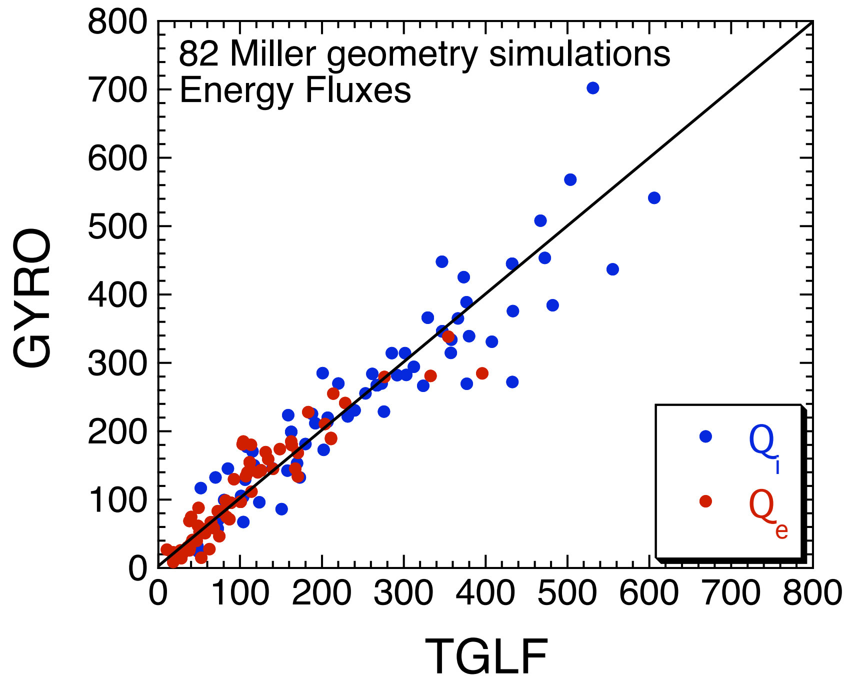

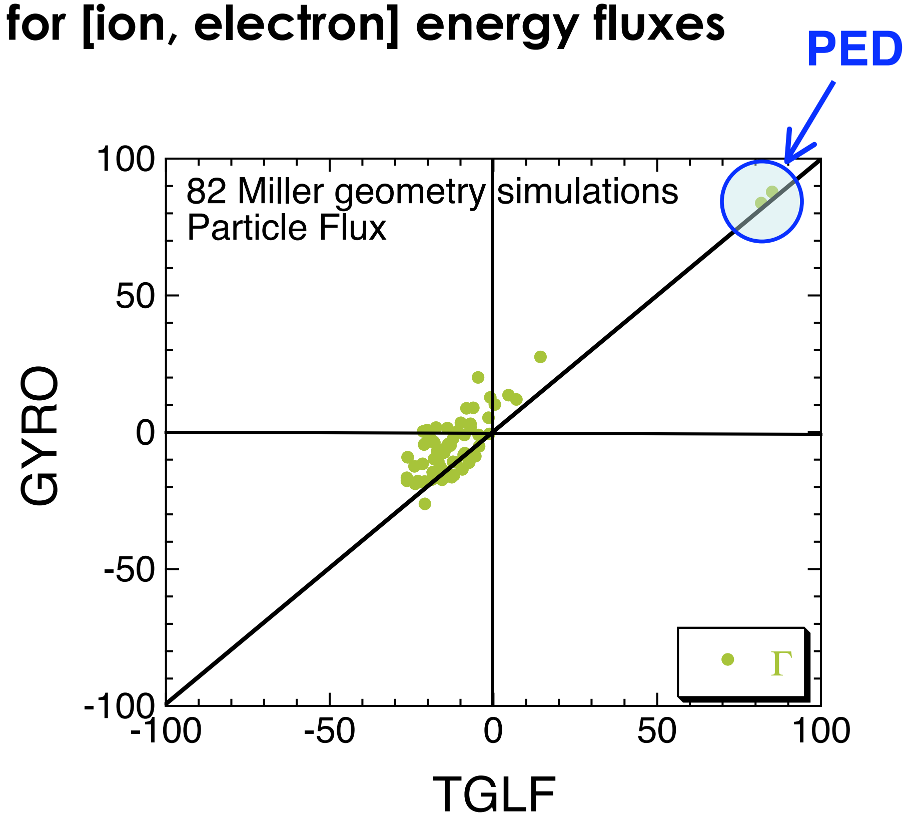

GLF23 fluxes are a poor fit to GYRO nonlinear shifted circle simulations

- **The RMS errors between GLF23 and GYRO for the 86 shifted circle cases are**

$$\sigma_{Q_i} = 42\%,\ \sigma_{Q_e} = 78\%,\ \sigma_{\Gamma} = 78\%,$$

- **GLF23 is systematically high, especially for the electron energy flux**

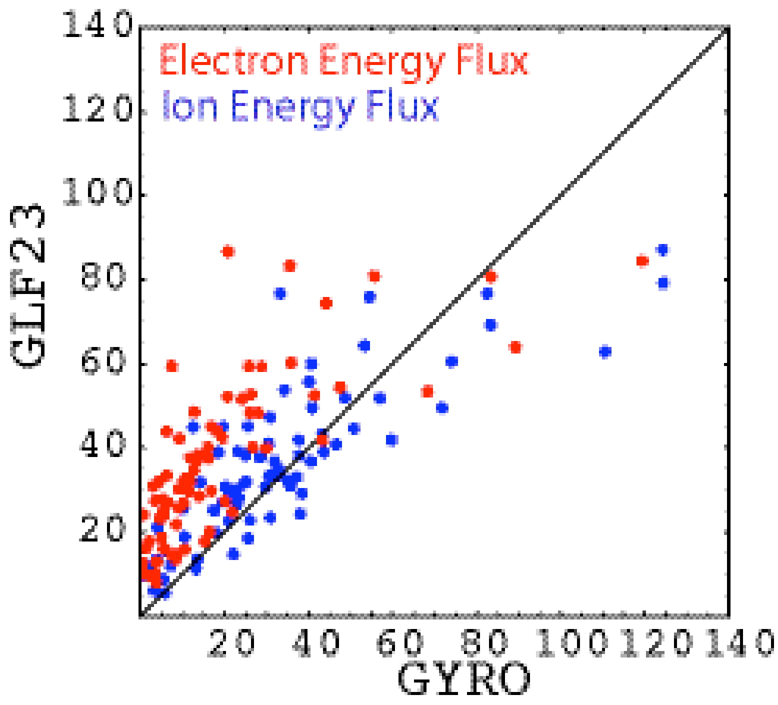

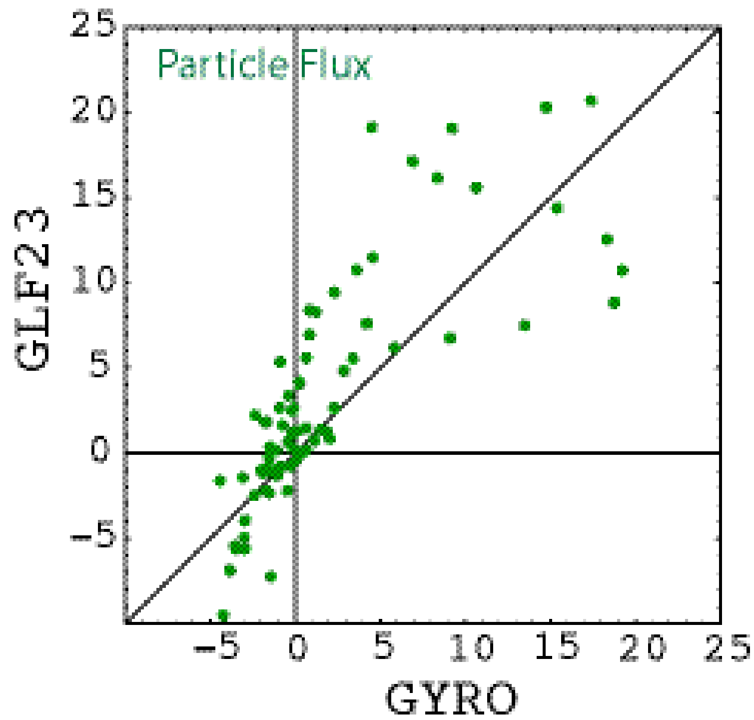

TGLF demonstrates better agreement with GYRO nonlinear simulations than GLF23

- **TGLF matches GYRO a/LT scan around GA-STD case with Miller geometry**
  - STD case: $R/a=3$, $r/a=0.5$, $q=2$, $s=1$, $a/L_T=3$, $a/L_n=1$, $\kappa=1.0$, $\delta=0$, $\beta=0$, $\nu_{ei}=0$
- **GLF23 low-k electron energy transport is systematically too large (red dashed line) and misses critical temperature gradient**
- **TGLF reproduces stabilizing effect of elongation seen in GYRO simulations**

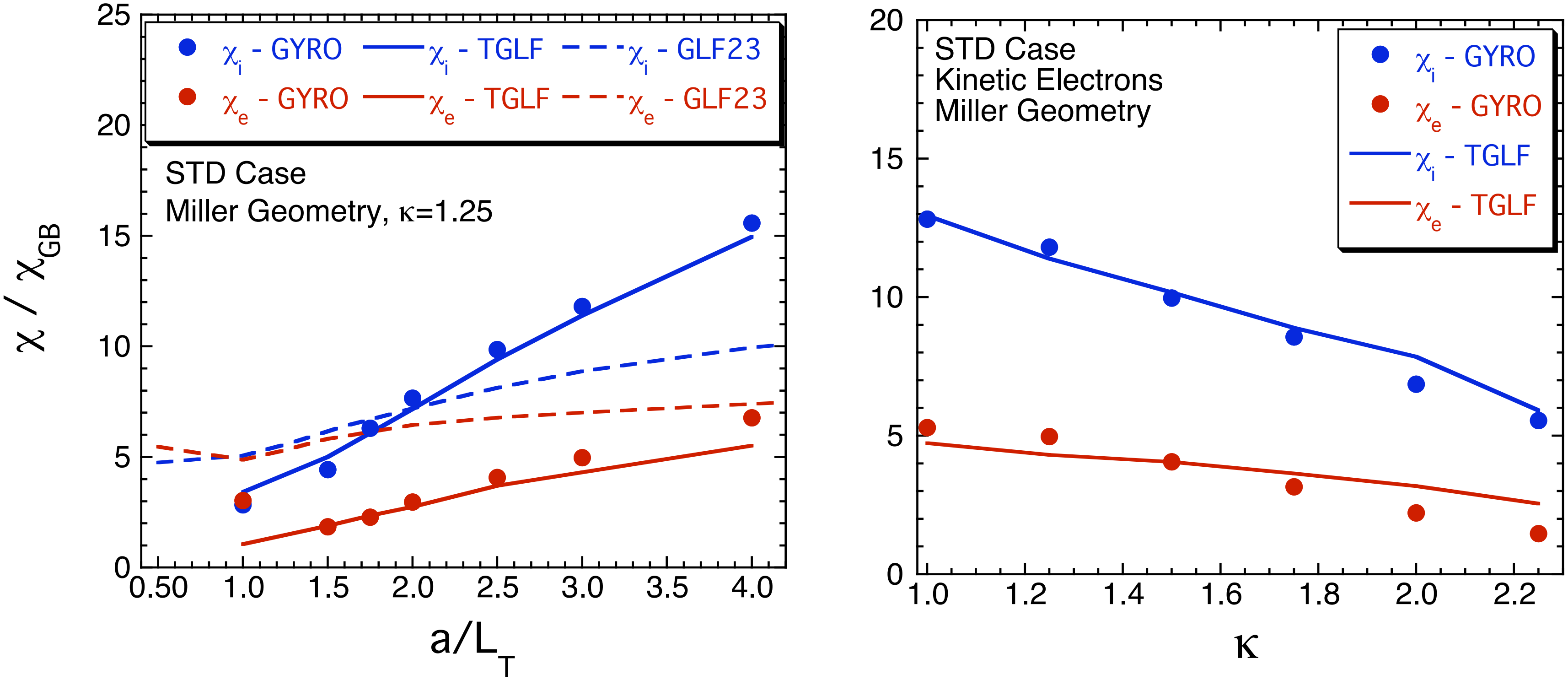

Linear ExB shear quench rule has been implemented in TGLF and shows good agreement with GYRO simulations

- **TGLF compared to GYRO ExB shear scans for STD case with Miller geometry, different values of κ, δ=0, low-k only, kinetic electrons** *
- **ExB shear rate with multiplier α_E is subtracted from maximum growth rate at each $k_\theta \rho_s$**

$$\hat{\gamma}_{net} = Max\left[\left(\hat{\gamma} - \alpha_E \hat{\gamma}_E\right)/\hat{\omega}_{d0}, 0\right]$$

Here,

$$\alpha_E = 0.3\sqrt{\kappa}$$

gives a good fit to GYRO ExB shear simulations with Miller geometry.

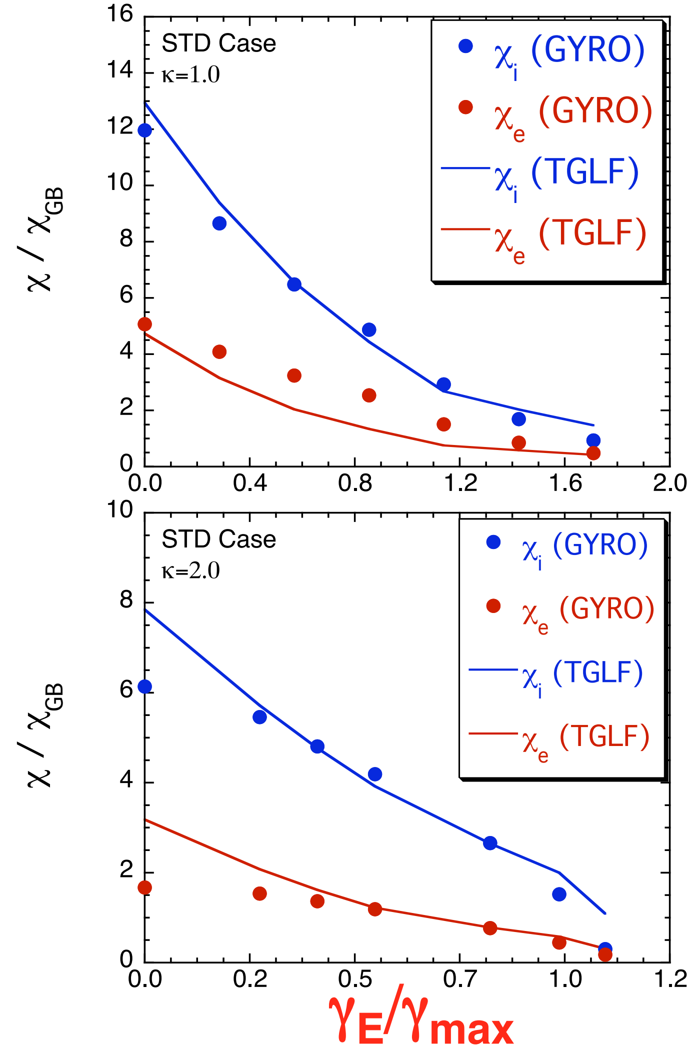

κ=1

κ=2

* See Kinsey, et al, Phys. Plasmas 14, 102306 (2007)

Validation of the TGLF transport model against experimental profile database

A profile database of 96 Discharges from DIII-D, JET, and TFTR has been assembled for model testing

- **The database is comprised of conventional L- and H-mode discharges**
  - 25 DIII-D L-, 33 DIII-D H-, 22 JET H-, 16 TFTR L-mode discharges
  - Most of JET and all of TFTR discharges in ITPA Profile Database
  - Most discharges are from parameter scans including ρ^*, ν^*, β, q, Ti/Te, v_ϕ
  - Only considered discharges with toroidal rotation (v_ϕ) data present
  - 96 shot database supplemented with DIII-D hybrid database (27 shots)
- **Simulation methodology**
  - TGLF and GLF23 run in the XPTOR transport code and treated equally with same solver and data
  - Predict core Te and Ti profiles for a single time-slice taking densities, toroidal rotation profiles, equilibrium, sources, sinks from experimental analyses
  - Boundary conditions enforced at ρ=0.84 for L-, H-modes
  - First TGLF runs are electrostatic with hydrogenic ions only
  - Chang-Hinton neoclassical, neoclassical poloidal rotation for ExB shear
  - TGLF simulations performed on local Linux cluster usually with 40 processors CPU time ≈ 10 mins for 40 grid pts, 40 processors

Validation metrics for testing against experimental data

- **Quantitative agreement measured by global and local figures of merit**

Avg. and RMS in the incremental stored energy W_{inc} for i^{th} discharge

$$\langle R_W \rangle = 1/N \sum_i W_{s,i} / W_{x,i} \qquad \Delta R_W = \sqrt{1/N \sum_i \left(W_{s,i} / W_{x,i} - 1 \right)^2}$$

ITER Physics Basis, CH 2, Nucl. Fusion 39, 2220 (1999)

RMS and offset for temperature T profile at each j^{th} radial pt for i^{th} discharge (same definition as used for benchmarking fluxes and growth rates)

$$\sigma_{T,i} = \sqrt{\sum_j \varepsilon_j^2} \Big/ \sqrt{\sum_j T_{x,i}^2} \qquad f_{T,i} = \frac{1}{N} \sum_j \varepsilon_j \Big/ \sqrt{\frac{1}{N} \sum_j T_{x,j}^2}$$

$$\varepsilon_j = T_{x,j} - T_{s,j}$$

Deviation between Exp. Temp (T_x) and Simulation (T_s)

Works for negative quantities like particle diffusivity, toroidal rotation

Avg RMS and offset for each dataset

$$\bar{\sigma}_T = \sqrt{\frac{1}{N} \sum_i \sigma_{T,i}^2} \qquad \bar{f}_T = \frac{1}{N} \sum_i f_{T,i}$$

TGLF exhibits lower average global errors than GLF23 for a large L- and H-mode profile database of 96 discharges

- **Database: 25 DIII-D L-,33 DIII-D H-, 22 JET H-, 16 TFTR L-mode discharges**
  - Supplemental DIII-D hybrid database = 27 discharges
- **Avg RMS errors in W_{inc} is 19% for TGLF, 36% for GLF23**
- **Offset in W_{inc} much smaller for TGLF (2% vs 16%)**
- **Avg RMS error in W_{tot} is ΔR_{Wtot}=10% for TGLF, 20% for GLF23**

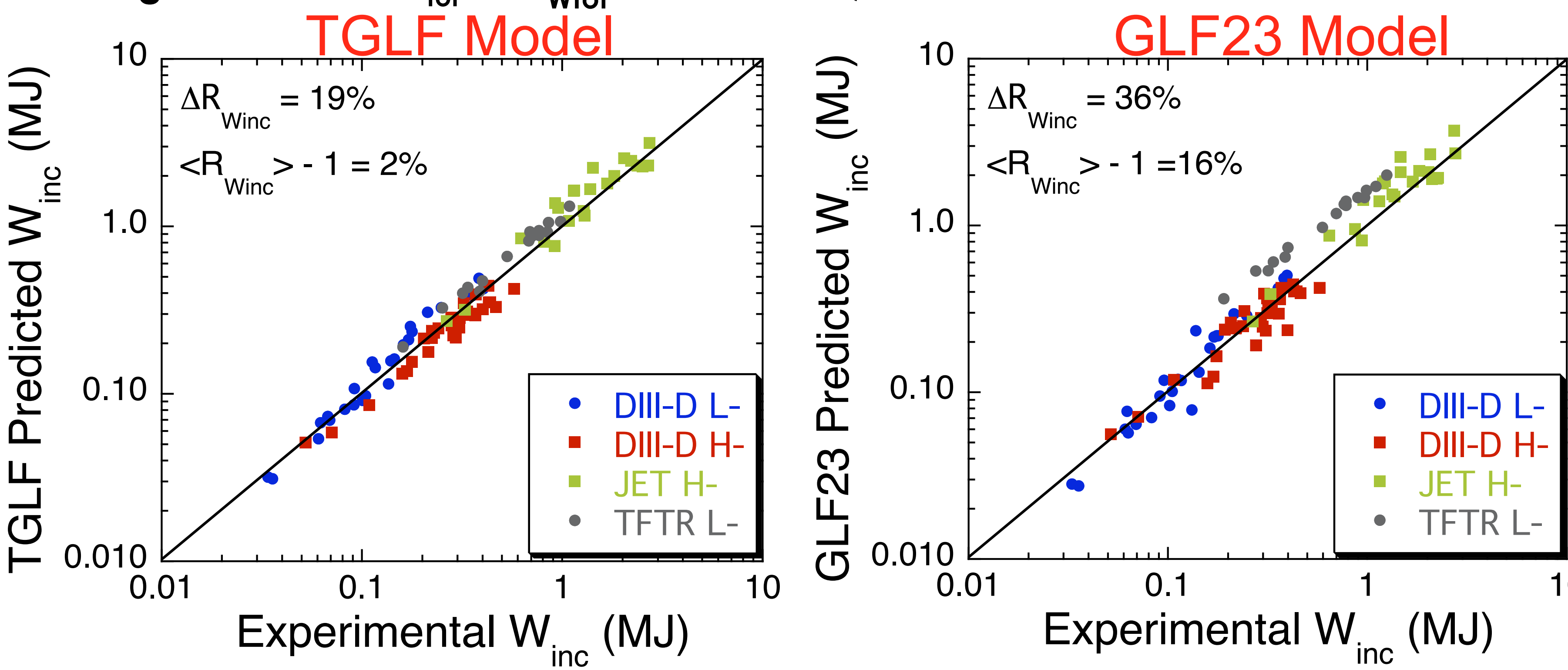

Local errors show TGLF model has fairly uniform agreement across DIII-D, JET, and TFTR discharges

- **Avg RMS error for [T_i,T_e] = [15%,16%]**
  - RMS errors in profiles computed outside q=1 to avoid influence by sawteeth
- **TGLF Avg RMS error for T_e smallest for H-modes, largest for DIII-D & TFTR L-modes**
- **TGLF has a small offset for DIII-D L- and H-modes and JET H-modes, but systematically overpredicts T_i,T_e for DIII-D and TFTR L-modes**

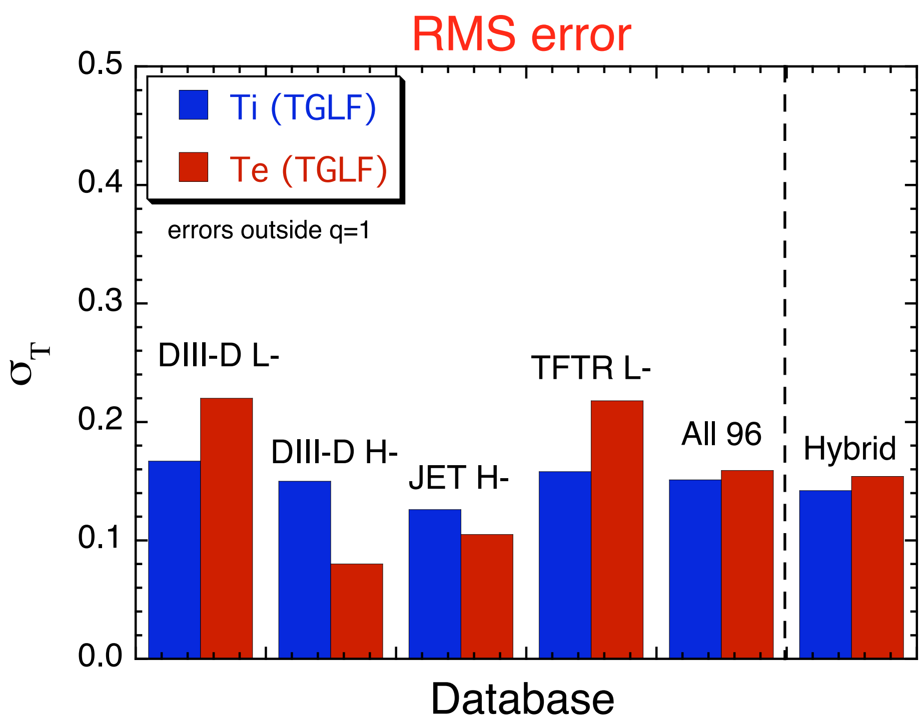

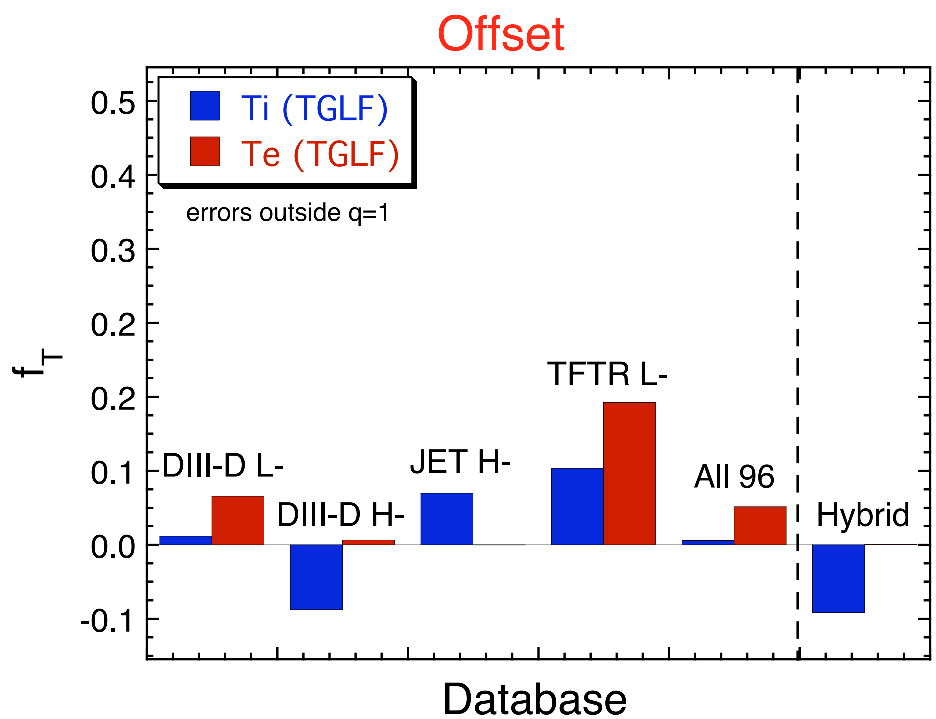

TGLF model has lower overall RMS errors and offsets in the temperature profiles than the GLF23 model

- **TGLF has avg RMS error for [T_i,T_e] of [15%,16%], GLF23 has [31%,23%]**
  - Comparable RMS errors for DIII-D L-, H-modes, and hybrids, but TGLF has noticably lower errors for JET and TFTR
- **TGLF has a smaller offsets JET and TFTR than GLF23**
- **TGLF has larger negative T_i offsets but smaller T_e offsets for DIII-D H-modes & hybrids**

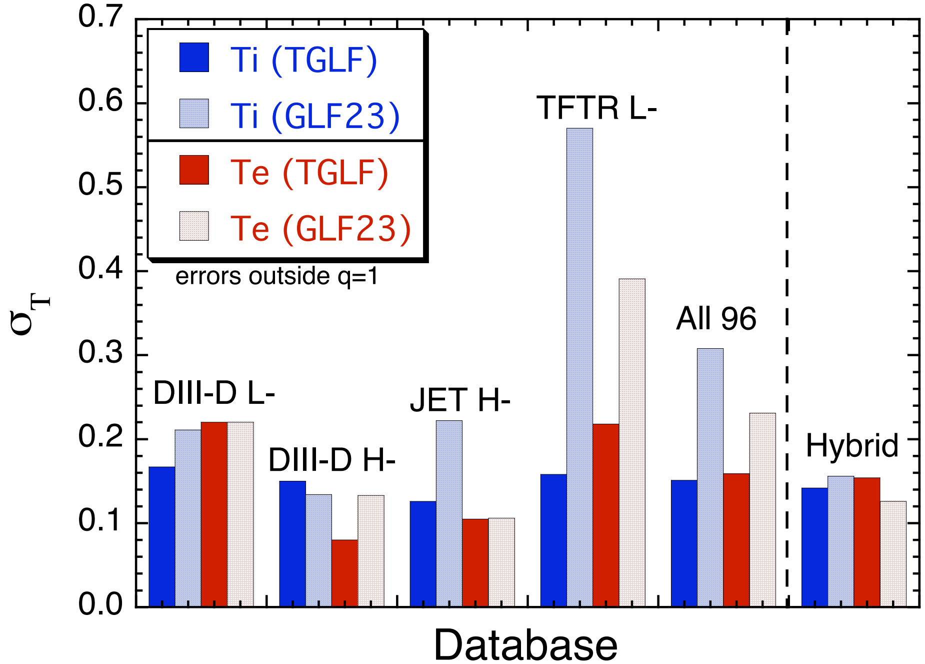

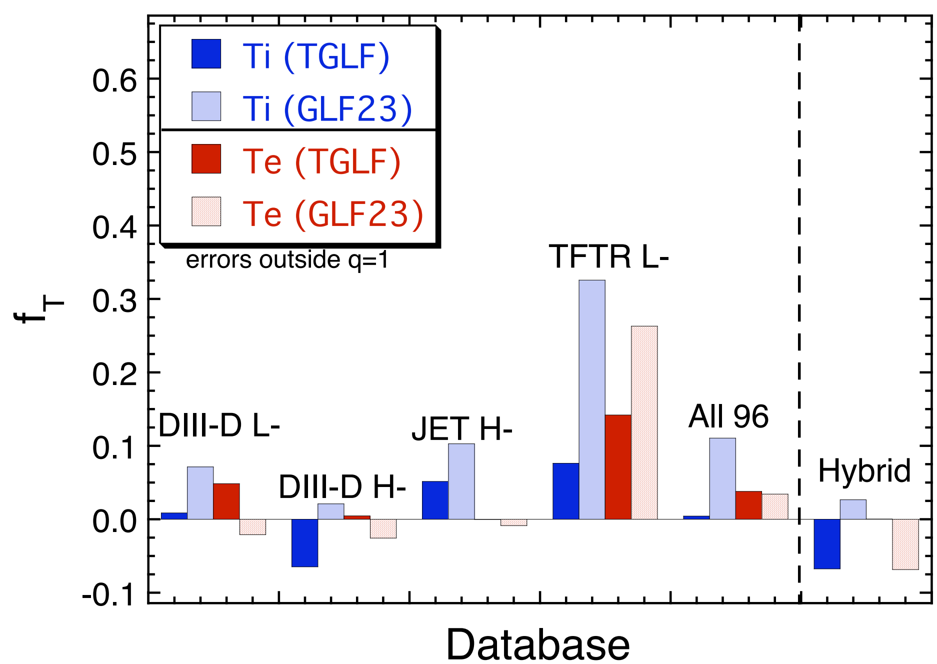

Sensitivity studies

Sensitivity to Boundary Conditions: TGLF simulations show L-mode profiles less sensitive to boundary temperatures than H-mode profiles for DIII-D

- **A measure of the sensitivity to the boundary temperature ("stiffness") is the ratio of the change in central temperature to the change in boundary temperature, $\Delta T_{io}/\Delta T_{BC}$**
- **The edge boundary temperatures were varied around the exp. values by +- 30% for a DIII-D H-mode and +-50% for a DIII-D L-mode**

H-mode: $\Delta T_{io}/\Delta T_{BC}$=0.20/0.30=0.67   L-mode: $\Delta T_{io}/\Delta T_{BC}$=0.07/0.50=0.14

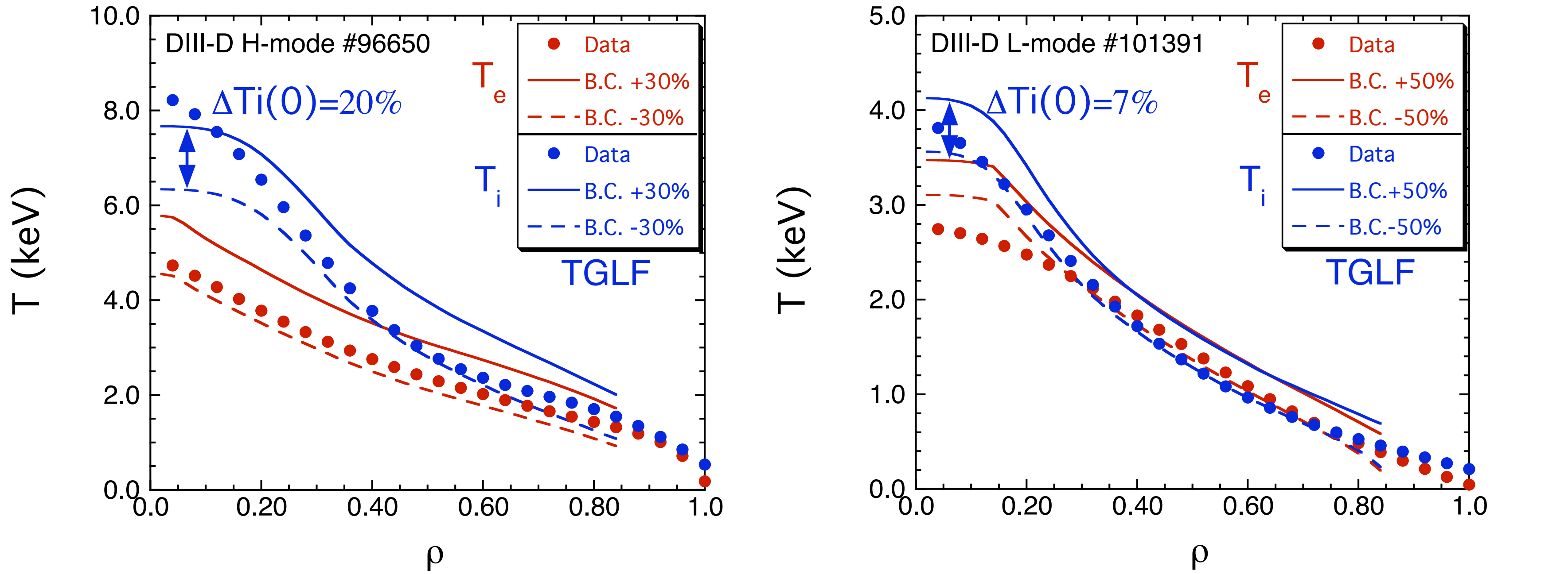

Sensitivity to Geometry: Miller geometry improves the agreement of TGLF with experimental profiles

- **Miller geometry yields very little improvement for shaped tokamaks (DIII-D, JET) but yields surprisingly noticeable improvement for TFTR which is circular**
  - Finite aspect ratio in Miller geometry increases transport in TFTR compared to s-α but is compensated by elongation in shaped tokamaks (DIII-D, JET)

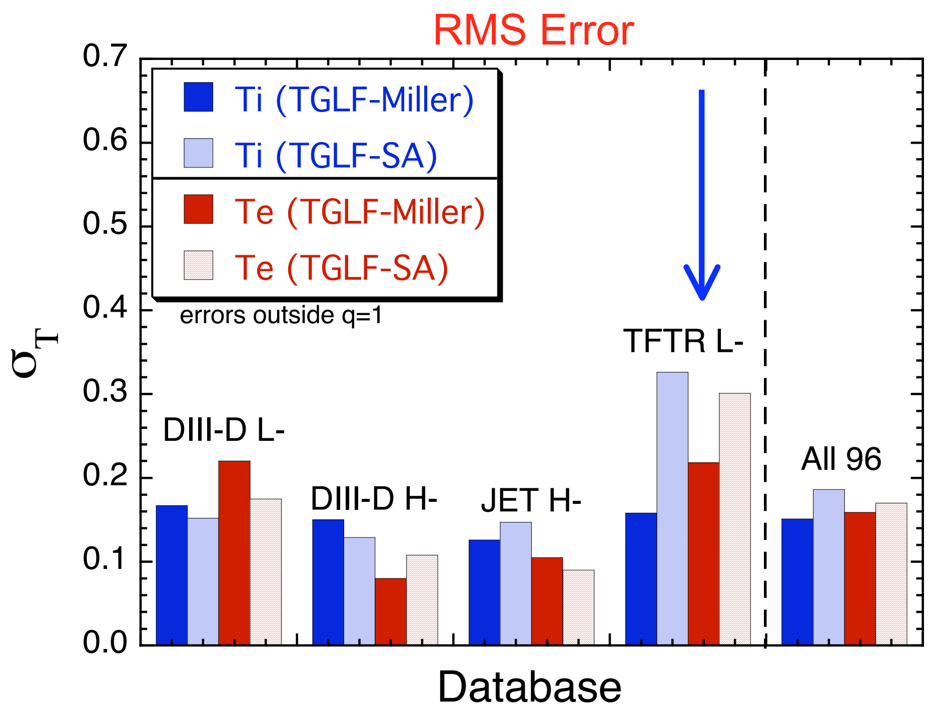

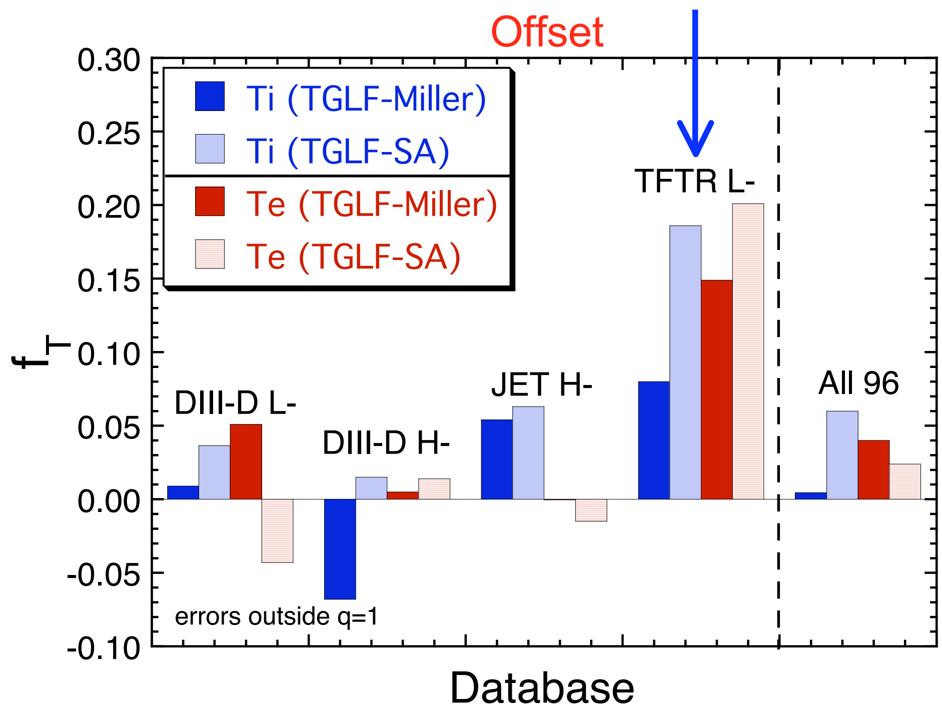

Transport is significantly higher for STD case going from s-α geometry to Miller geometry with κ=1.0

- **GYRO simulations varying r/a for STD case show larger χ's with Miller finite aspect ratio geometry compared to infinite aspect ratio s-α geometry**
  - Elongation shear (and elongation) stabilization compensates for this in DIII-D
  - GYRO κ=1.5 results for χ_i close to s-α result, χ_e still higher than s-α
  - Assumed $s_\kappa=(\kappa-1)/\kappa$ for elongation shear

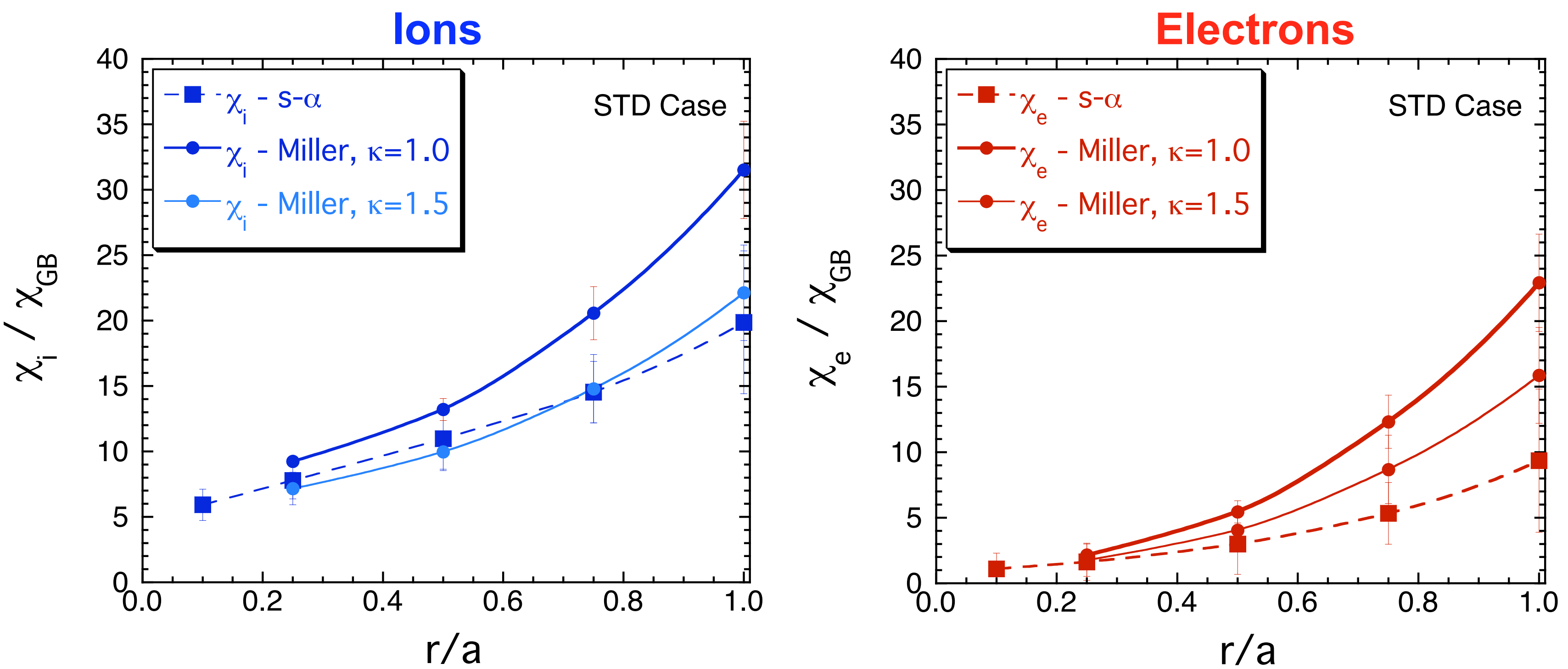

Elongation shear is more stabilizing than just the local κ

- **Miller shaped finite aspect ratio equilibrium model depends on both κ and s_κ**

$$s_\kappa = \frac{r}{\kappa}\frac{\partial \kappa}{\partial r} \cong \frac{\kappa - \kappa_o}{\kappa}$$

where κ_o is the central κ value

κ only, no elongation shear **elongation shear only, κ fixed**

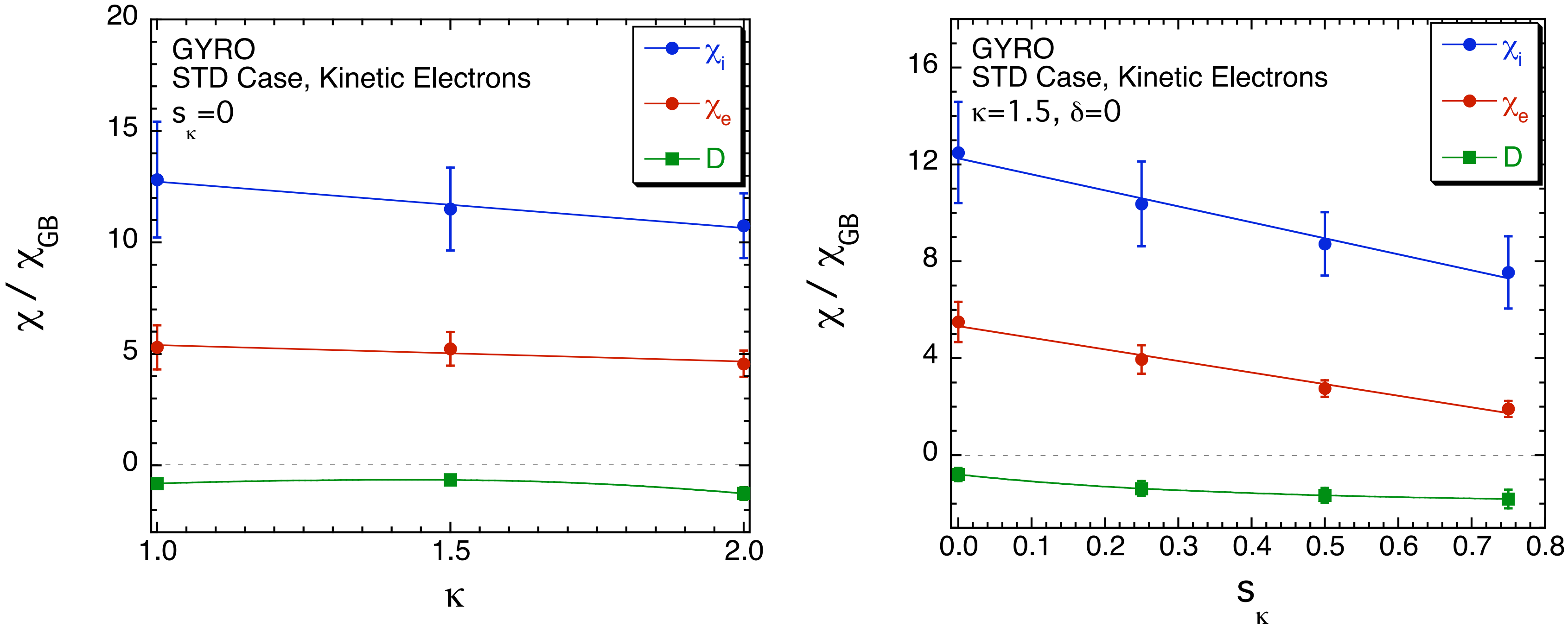

Sensitivity to ExB Shear: TGLF with ExB shear quench rule reproduces the observed change in transport in a DIII-D hybrid rotation scan

- **Toroidal rotation varied by 3x, beam power changed to keep β fixed (Politzer APS07 talk)**
- **TGLF shows ExB shear more important in high rotation case**
- **ExB shear has much less impact on T_e for hybrids because the electron transport is dominated by high-k modes**

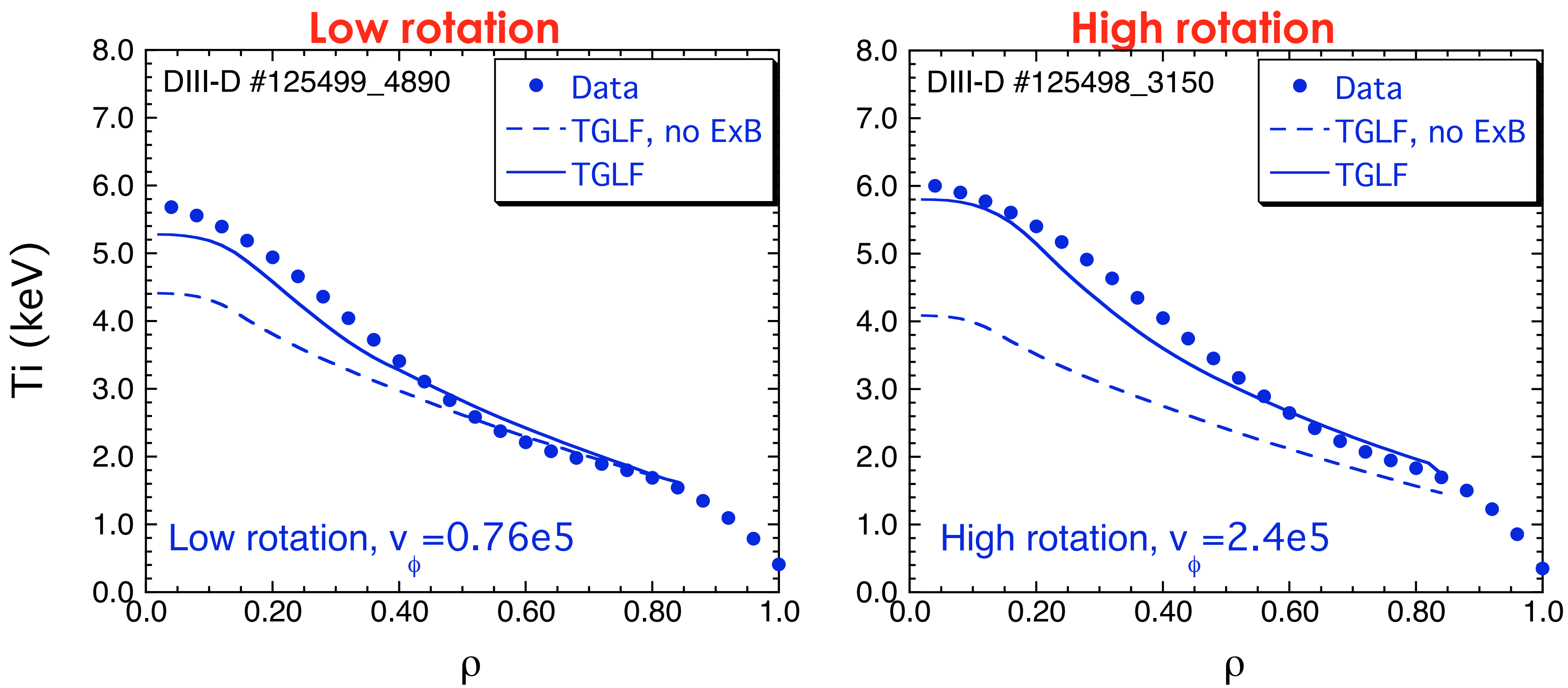

Sensitivity to ExB Shear: TGLF with ExB shear quench rule reproduces the observed change in transport in a DIII-D hybrid rotation scan

- **Toroidal rotation varied by 3x, beam power changed to keep β fixed (Politzer APS07 talk)**
- **TGLF shows ExB shear more important in high rotation case**
- **ExB shear has much less impact on T_e for hybrids because the electron transport is dominated by high-k modes**

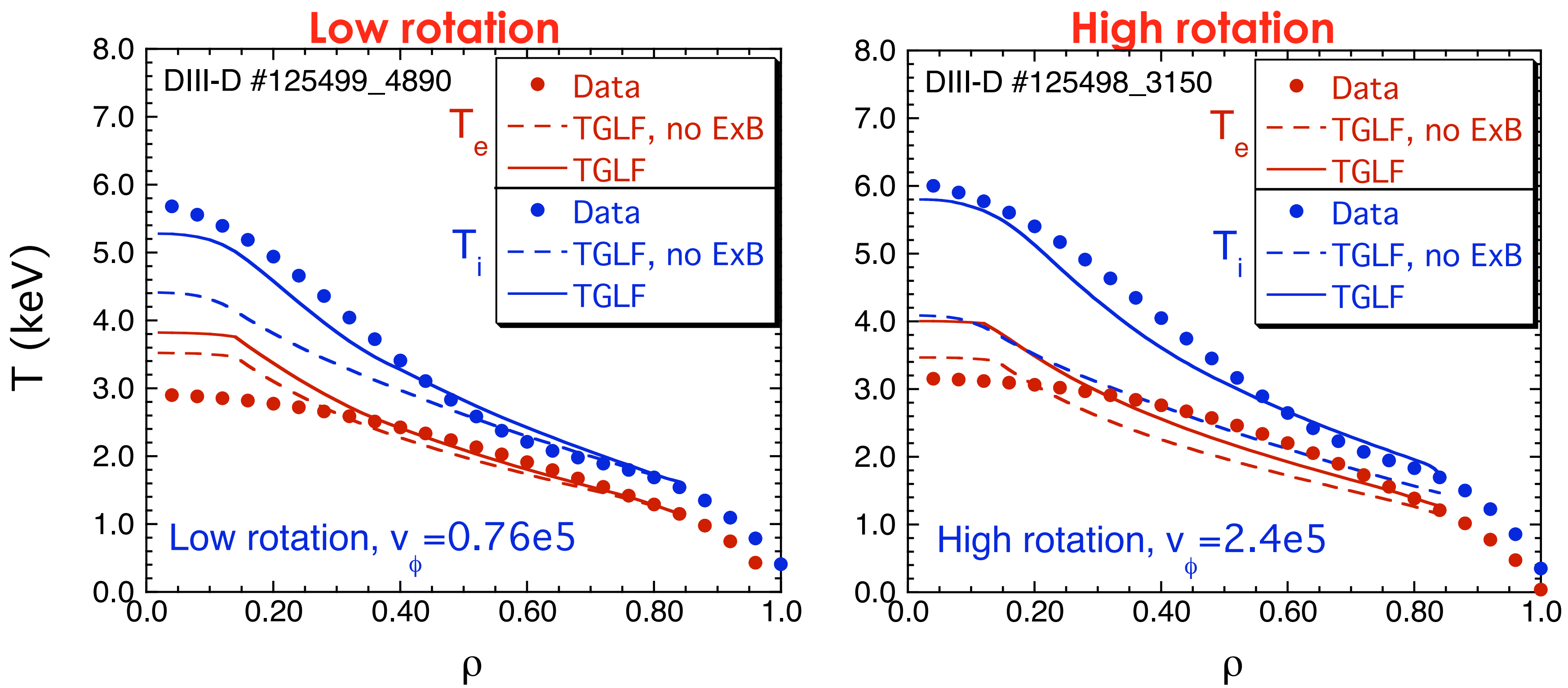

Sensitivity to ExB Shear: TGLF results also show that ExB shear is less important in low q95 hybrid discharges

- **Toroidal rotation varied by 2x in hybrid pair w/ q_{95}=3.1**
  - q_{95}=5.0 for discharge pair on previous slide
- **Like high q_{95} pair, ExB shear more important in high rotation case**
- **Modeling of 10 low and high q_{95} shots shows TGLF tends to underpredict the profiles for high q_{95} and overpredict the profiles for low q_{95}**

Low rotation

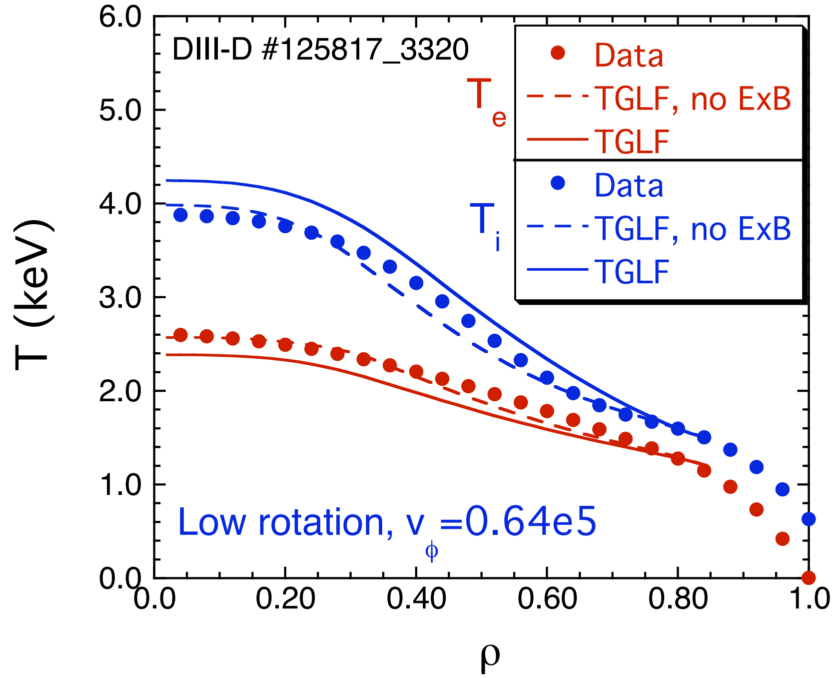

High rotation

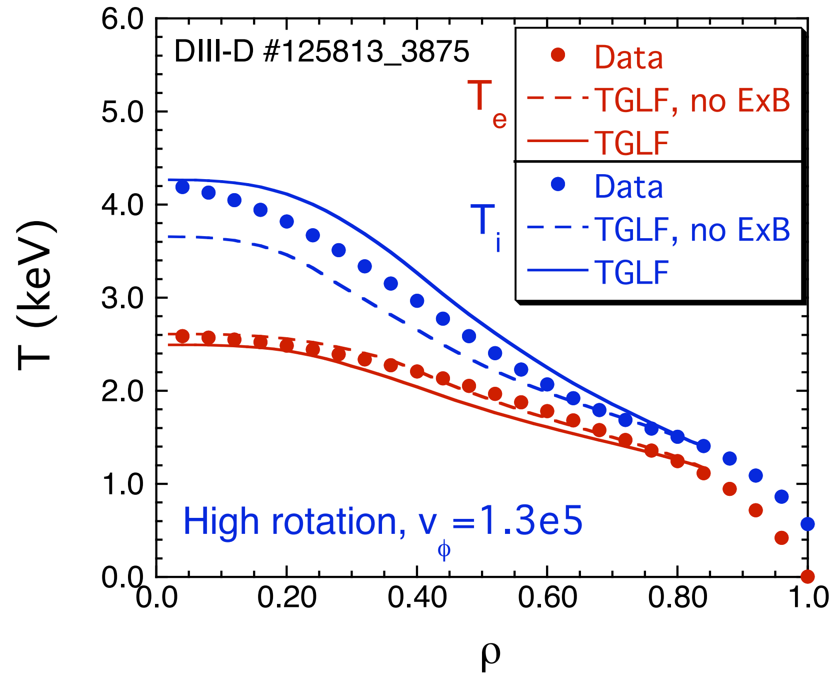

Sensitivity to ExB Shear: DIII-D disharges have been modeled with TGLF using E_r Data to compute the ExB shear

- **TGLF modeling of DIII-D discharges using experimental radial electric field data yields approximately the same predicted temperatures as those obtained computing ExB shear with neoclassical poloidal velocity**
- **15 L- and H-mode discharges modeled w/ E_r data**
- **More noticable differences may appear in ITBs and H-mode pedestal regions**

γ_E using model v_θ

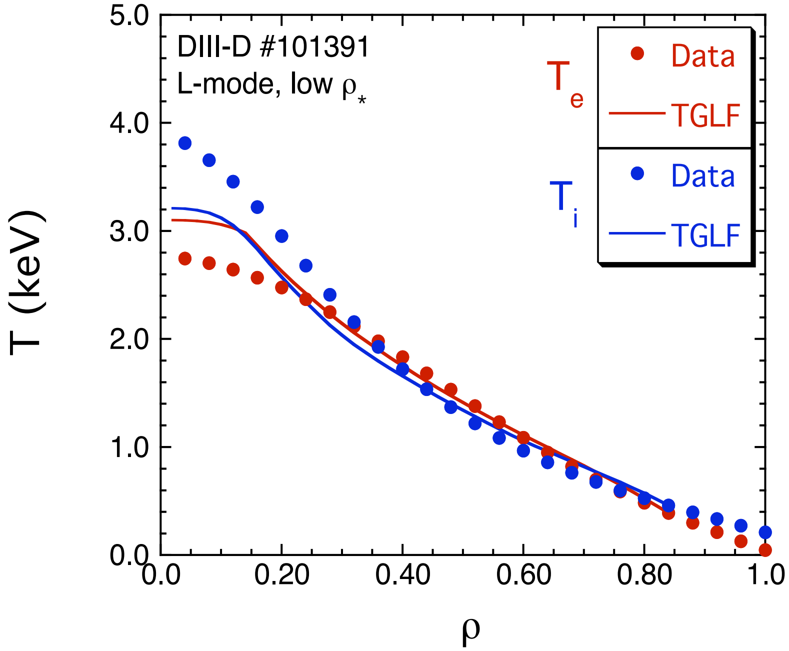

γ_E using E_r data

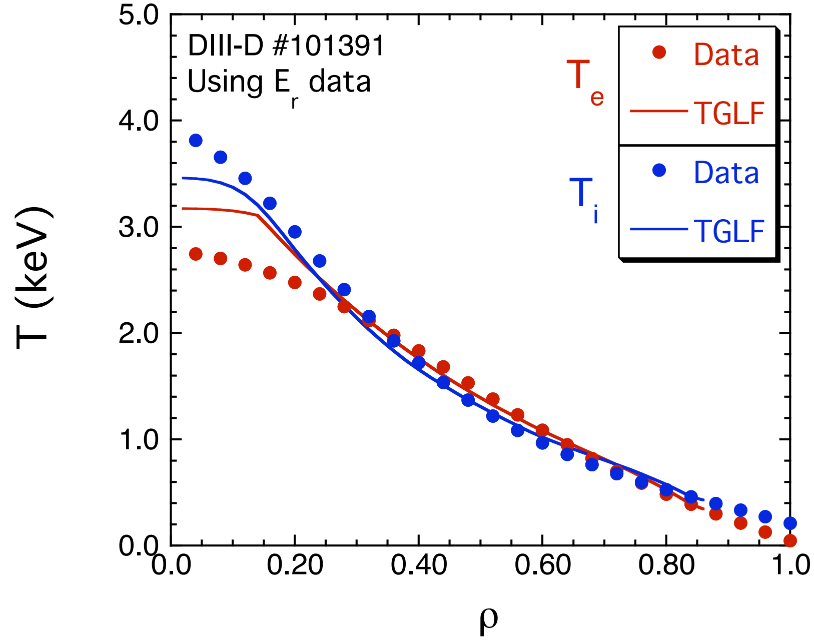

Sensitivity to High-k Modes: TGLF predicts high-k modes can dominate the electron transport in the plasma core

- **ETG coefficient in saturation rule determined by fitting GYRO simulation of GA STD case where $\chi_{e,high\text{-}k}$ / $\chi_{e,total}$ = 11% (k_y > 1, μ=30)**
- **TGLF has lower low-k contribution to χ_e than GLF23**
- **Suppression of ITG/TEM transport by ExB shear results in high values of $\chi_{e,high\text{-}k}$ / χ_e as χ_i approaches neoclassical**
  - Low q_{95} hybrids have largest $\chi_{e,high\text{-}k}$ / χ_e , L-modes have lowest $\chi_{e,high\text{-}k}$ / χ_e

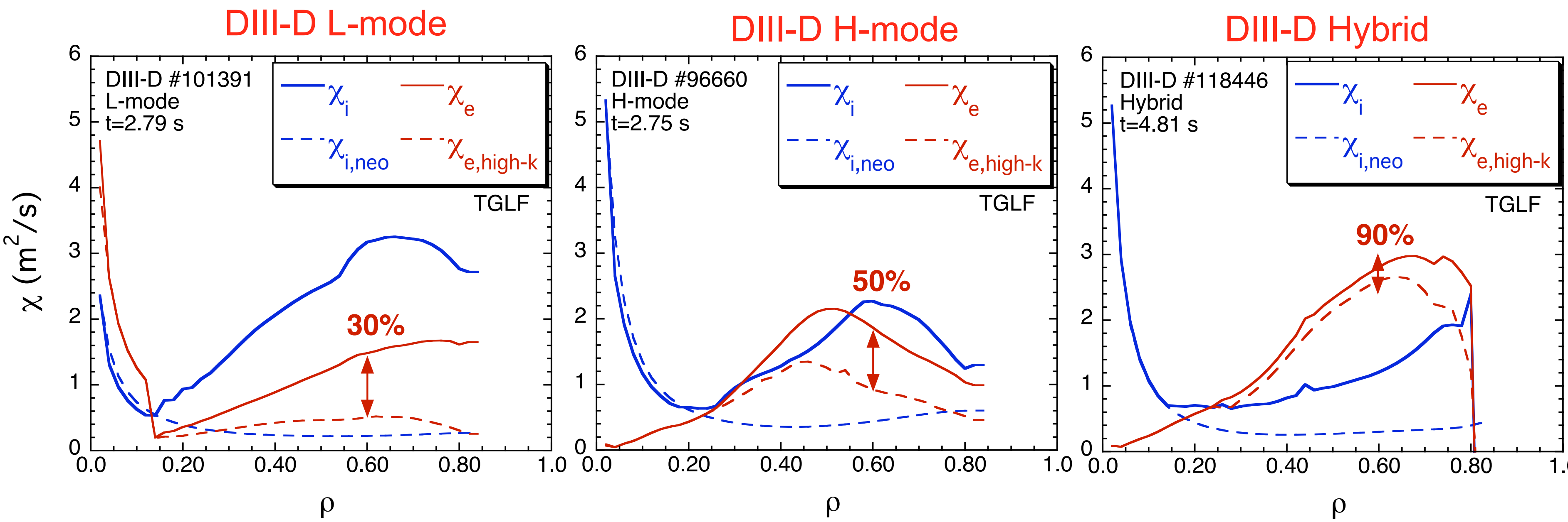

Sensitivity to Density Evolution: TGLF reproduces peaked density profiles and has low RMS errors for database

- **Density evolved along w/ Te, Ti with feedback on wall source to match line avg. density using the impurity, fast ion densities from exp. analyses**
  - Avg. σ_{ne} = 12% for 96 discharge database
- **RMS error in [Ti,Te] virtually unchanged from [15%,16%]**

Avg. σ_{ne}, f_{ne} for q>1

DIII-D L-	8 %, +1.2%
DIII-D H-	12 %, +8.0%
JET H-	16 %, +8.3%
TFTR L-	9 %, +3.4%

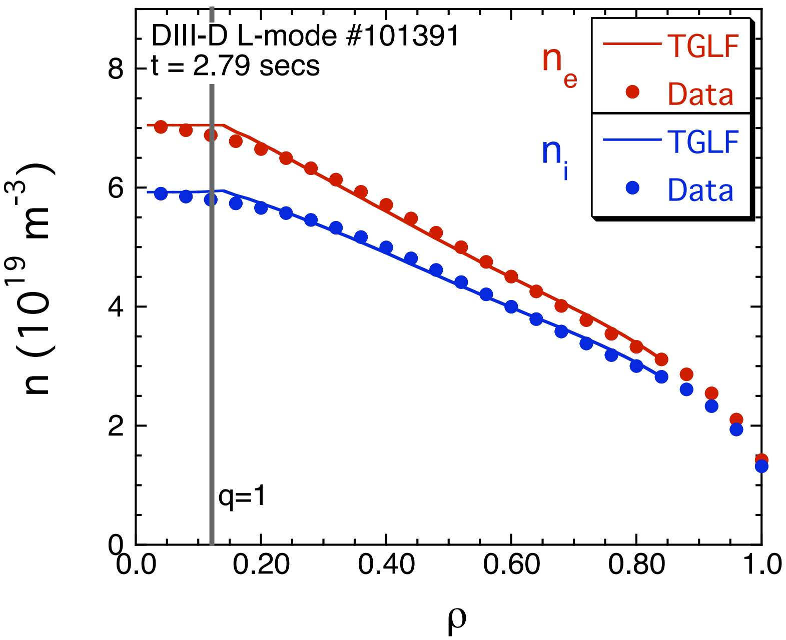

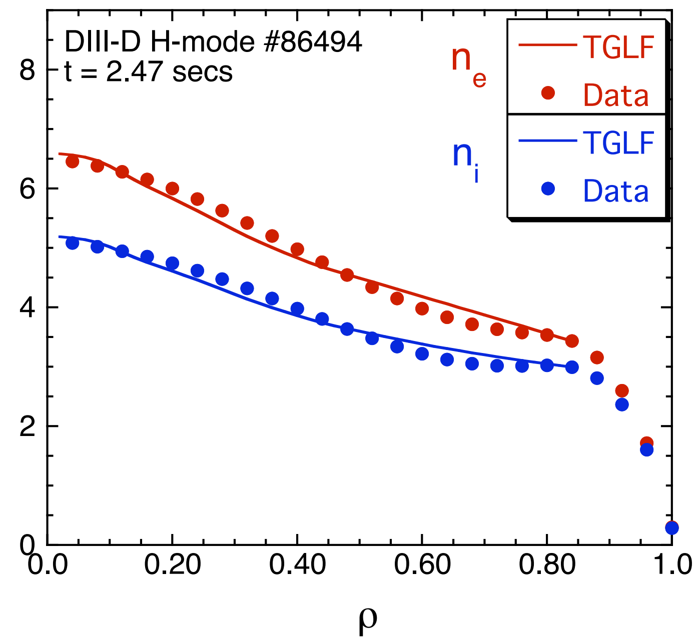

Sensitivity to Finite Beta: Finite β found to be mildly stabilizing in the plasma core of discharges in database

- **For STD case, energy fluxes decrease with β, then increase above ideal limit**
  - Magnetic flutter contribution not agreeing with GYRO, further work needed
- **RMS in T_i for hybrids decreases from 15% to 12% with finite β, smaller change in rms errors for DIII-D H-mode database**

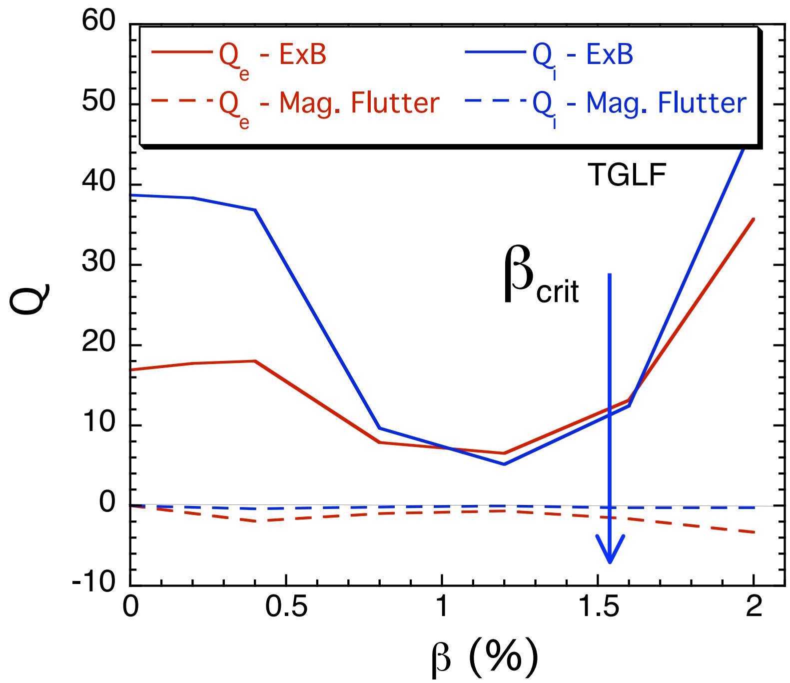

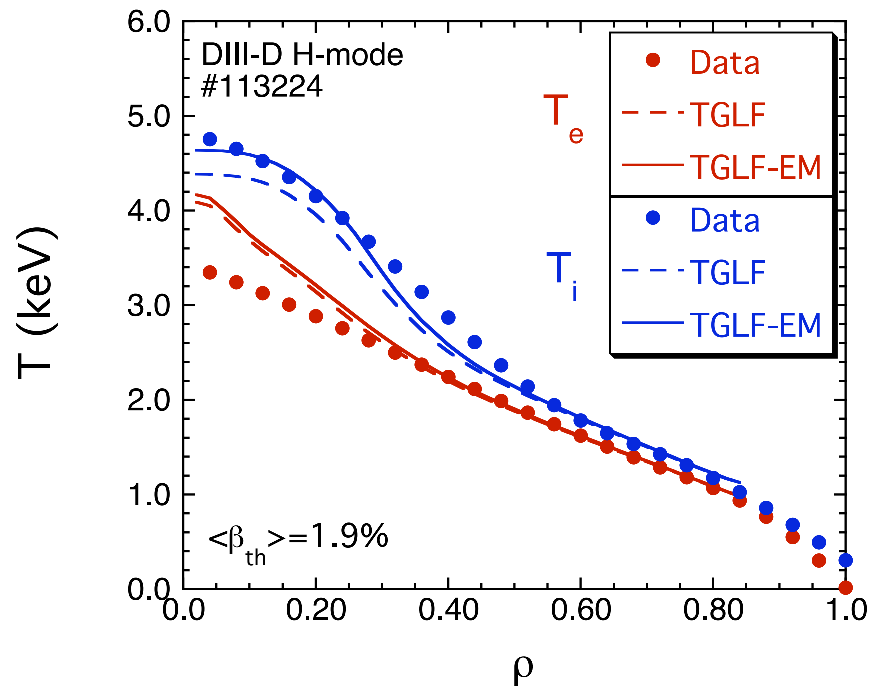

TGLF Typically Underestimates Transport In Near Edge Simulations of DIII-D L-mode Discharges

- **Boundary conditions have been extended to ρ=0.96 with Te, Ti predicted**
  - Nearly a dozen DIII-D L-mode discharges modeled
  - Predicting the density also for #101391 did not alter the temp. profile predictions
- **More TGLF and GYRO comparisons needed for L-mode edge conditions**

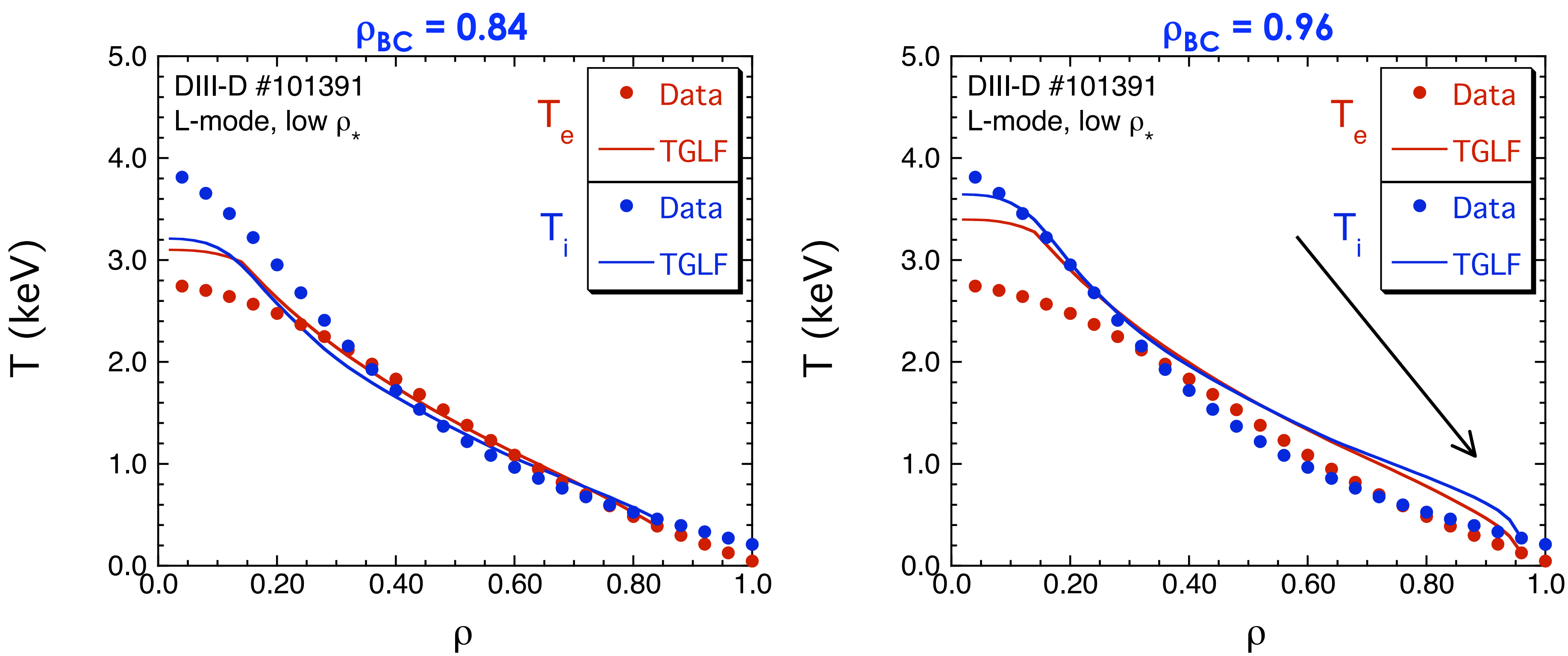

TGLF shows good agreement with GYRO Miller geometry low-k simulations for large values of r/a

- **R/a held fixed along with other local quantities, essentially a scan in trapped fraction, r/R**
  - r/R = (r/a) / 3 since R/a=3.0
- **Where is the missing transport coming from ?**
  - TGLF agrees w/ GYRO for STD case parameters, but s > 2 typical at ρ>0.75 for DIII-D

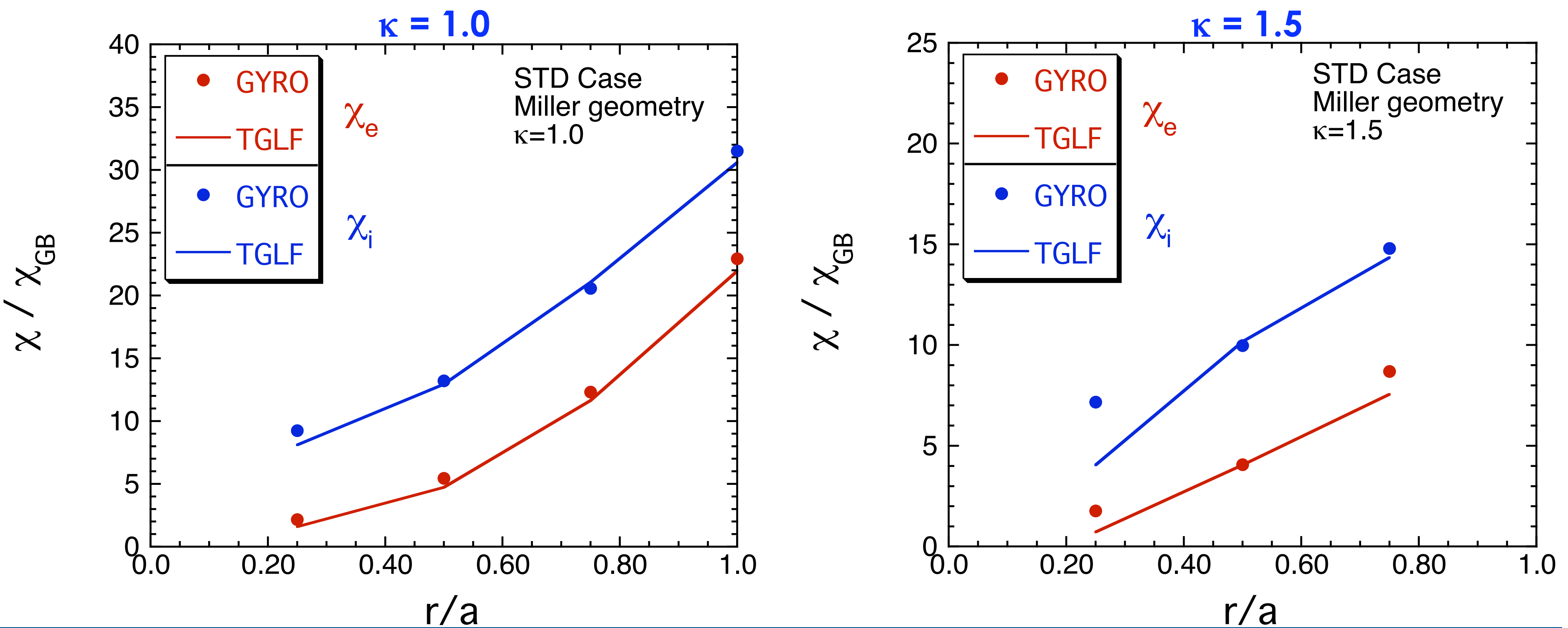

TGLF overpredicts central Te profile in DIII-D discharges with density peaking

- **High q95 hybrid cases show more density peaking than low 95 cases in this group of DIII-D shots**
- **ETG threshold is sensitive to a/Lne**
  - Peaking decreases transport

Experimental Density

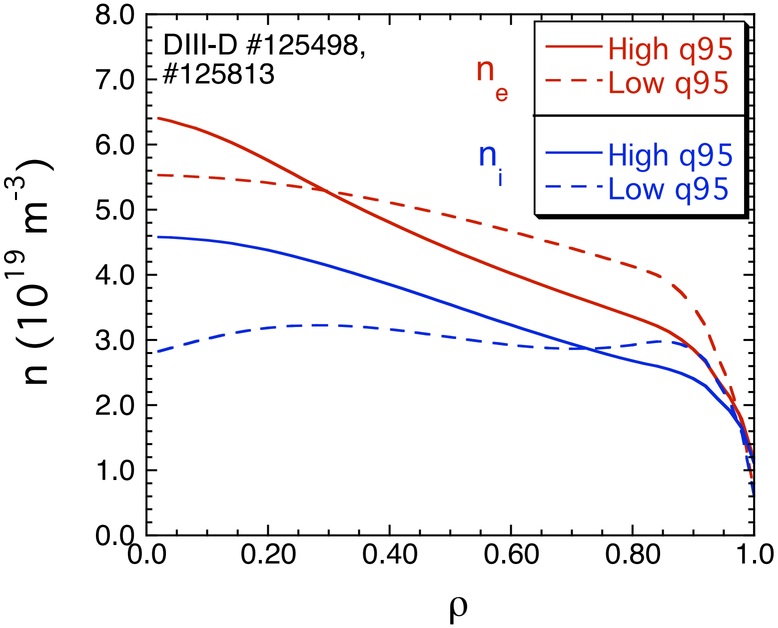

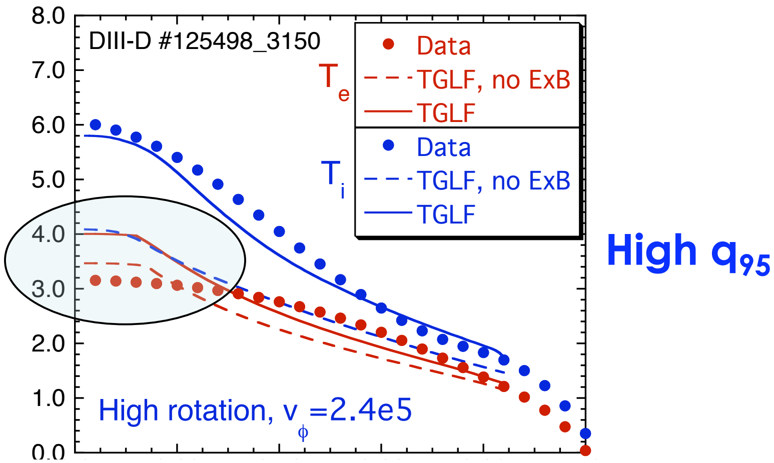

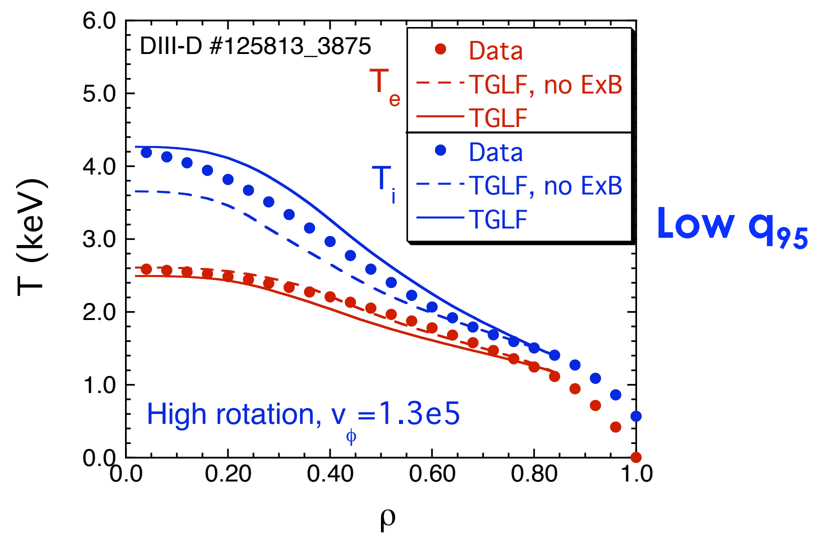

Only temp. profiles evolved

Insufficient Particle Transport Close To Magnetic Axis in DIII-D Hybrid Discharges With Low ITG/TEM Transport

- **Neoclassical particle transport taken to be equal to χ_e neoclassical**
  - D_{neo} enhanced to 20 χ_e neoclassical when q<1
- **Central density profiles overpredicted in DIII-D hybrid discharges with strong ExB shear stabilization**

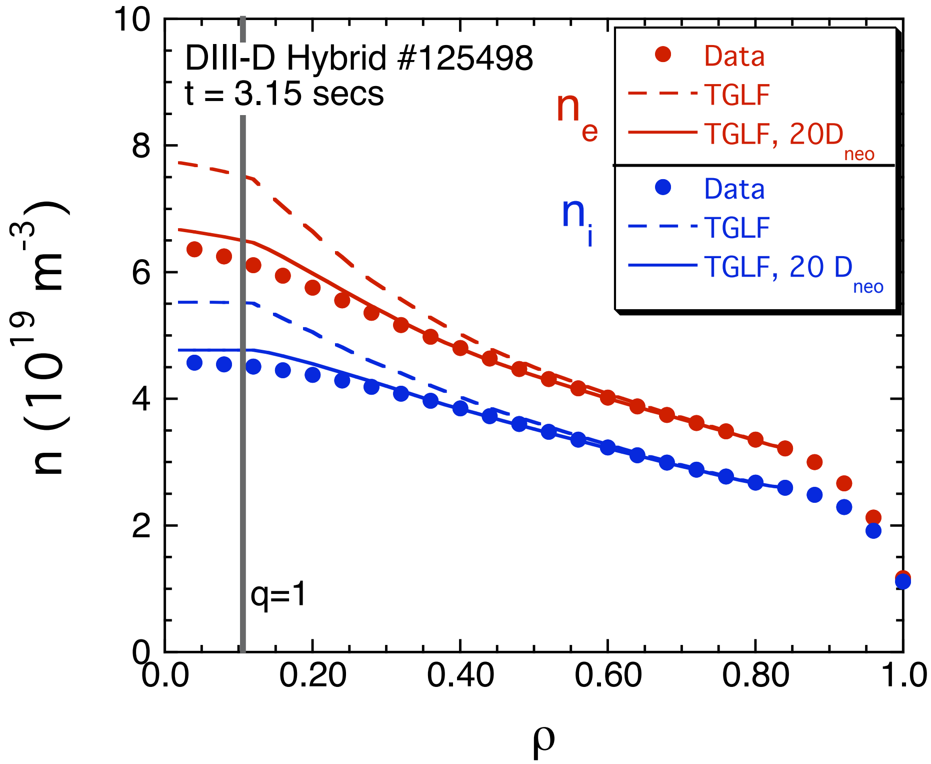

Summary

- **Quasilinear saturation rule in TGLF shows remarkable agreement with large GYRO transport database of 83 simulations with Miller geometry !**
- **An ExB shear quench rule has been implemented in TGLF that fits GYRO nonlinear simulations at various elongations**
  - Quench rule well validated by rotation scans in DIII-D hybrid database, ExB shear more important in high rotation cases and high q95 cases
- **Better fit to theory (GYRO) resulted in better predictions of exp. data**
  - Comparison between the TGLF and GLF23 models for a database of 96 discharges from DIII-D, JET, and TFTR shows that TGLF exhibits 19% [2%] RMS [offset] error in Winc versus 36% [16%] for GLF23
  - Over 500 transport runs !
- **Average RMS errors in [T_i,T_e] are [15%,16%] for TGLF, [31%,23%] for GLF23**
- **TGLF predicts the high-k/ETG modes dominate the electron energy transport when the ion energy transport approaches neoclassical**
  - ETG dominant contributor to χ_e in DIII-D hybrid discharges
  - High-k modes predicted to be important in the deep core of L- and H-modes
- **TGLF accurately predicts density profile shapes with an average RMS error of 12% for 96 discharge database**

Where do we go from here?

- **Modeling/Theory**
  - Include parallel velocity shear in TGLF equations, predict momentum transport including ITB discharges and intrinsic rotation cases
  - Study kinetic impurity effects in TGLF (see Staebler's poster)
  - More GYRO and TGLF studies needed
    - L-mode near edge conditions (e.g. high magnetic shear, high collisionality)
    - More ETG simulations for various conditions using Miller geometry
  - Extend modeling toward edge region
    - Move from Miller equilibrium model to actual equilibria (e.g EFITs)
  - Why are H-modes systematically overpredicted and L-modes underpredicted ?
  - Deep core ETG transport sensitive to core density profile (e.g. DIII-D hybrids)
  - Rescale CX and ionization flows as wall neutral source is rescaled
  - Test model with high beta and for low aspect ratio (NSTX and MAST)
  - Model perturbative experiments (e.g modulated ECH)
  - Improve sawtooth model in transport code
  - More accurate neoclassical particle transport needed (i.e. near axis)
  - Replace ExB shear rule with rotational ballooning mode net linear growth rate model; χ vs γ_E curve changes shape with aspect ratio
  - Include nonlocal effects, small effect of turbulent exchange
  - Revisit ITER projections

Where do we go from here?

- **Experimental analyses**
  - In general, we need the highest standard of data analysis
  - C-mod data
  - Kinetic EFITs
  - Accurate fits to raw data near edge
  - Improve assessment of error bars
  - Scrutinize sources (particle, energy)
  - Examine effects of atomic physics
  - Other possible data issues:
    - MHD activity
    - time derivative terms
    - fast ion losses
    - beam deposition
    - dilution

Backup slides

Agreement can also be quantified using raw experimental data points and computing a reduced χ^2

- **RMS errors and offsets we have used compare the model predictions with fitted experimental profiles**
  - Doesn't take into consideration scatter in raw data as well as the error bars in the data
  - Doesn't distinguish between older and newer (often less scatter, smaller error bars) data
- **Reduced χ^2 values used to quantify fits to raw data**

$$\chi^2 = \frac{1}{N}\sum_j \frac{\varepsilon_j^2}{\sigma_{bar,j}^2}$$

where σ_{bar}=raw data error bar for j^{th} radial pt

	χ^2_{TGLF}	χ^2_{Fit}	σ_{rms}
Te:	3.96	2.0	0.05
Ti:	1.37	2.4	0.11

- **Reduced χ^2 varies depending on size of error bars**

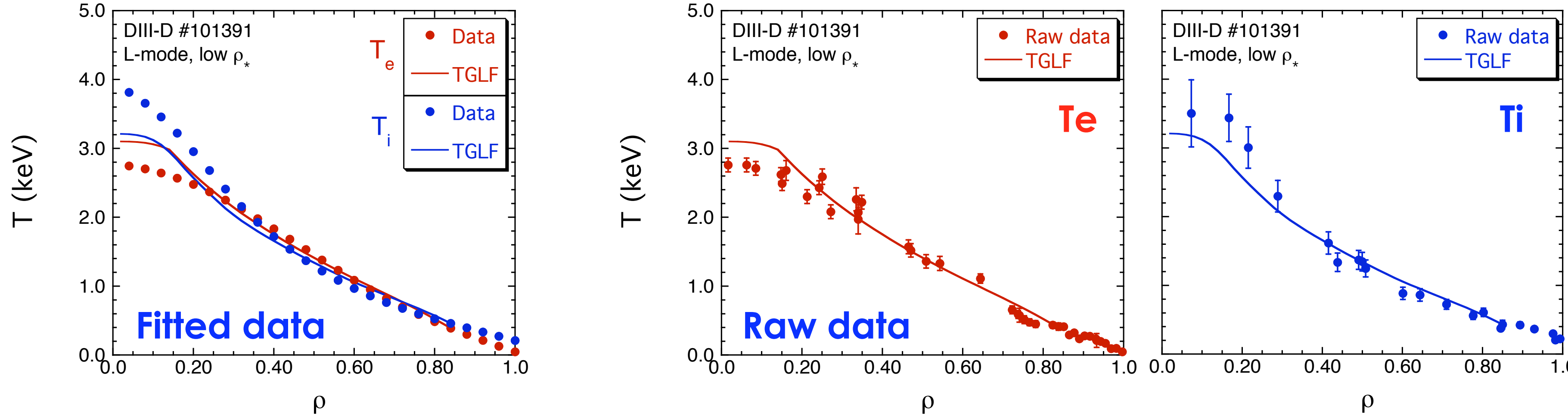

TGLF reproduces observed change in confinement as the toroidal rotation varies in a TFTR torque scan

- **Toroidal velocity varied by changing mix of co- and ctr- NBI**
- **Less NBI power needed in high rotation cases to achieve same stored energy as low rotation cases at same density**

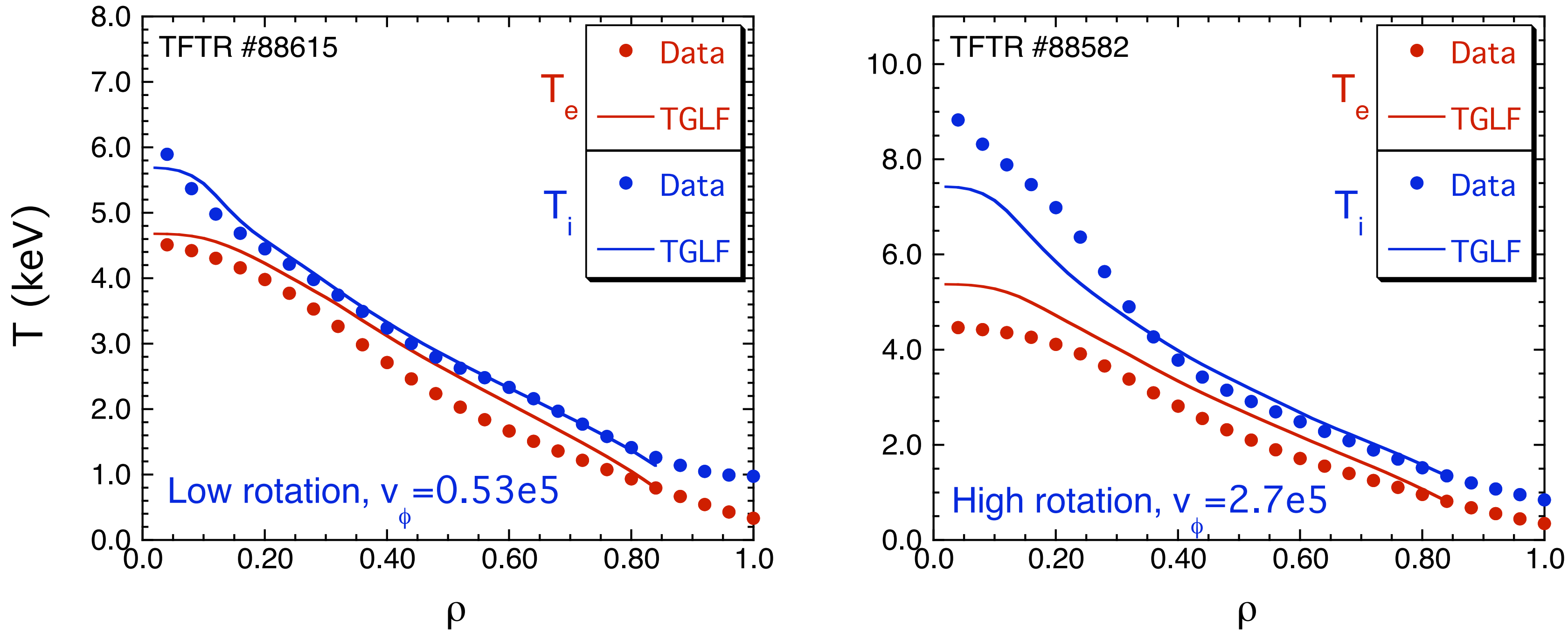

Linear GKS Database for TGLF Testing

Scan	Set	Scan type	# pts
1	STD	ky scan (0.01→ 0.70) @ various q (1–5)	80
2	STD	shear scan (-1→ 2) @ various q (1–5)	55
3	STD	shear scan (-1→ 2) @ various q (1–5), α=1	55
4	STD	ky scan (0.01→ 0.70) @ various a/L_T (2 → 5)	64
5	STD	ky scan (0.01→ 0.70) @ various T_i/T_e (0.5 → 2.0)	64
6	STD	a/L_T scan (0 → 3) @ various a/L_n(1 → 2)	80
7	STD2	ky scan (0.75→ 3.0) @ various q (1–5)	80
8	STD2	shear scan (-1→ 2) @ q=1.2,1.4,1.6	64
9	STD2	shear scan (-3→ 3) @ q=2,4	32
10	STD2	shear scan (-1→ 2) @ various q (1–5), ky=0.15	55
11	STD2	shear scan (-1→ 2) @ various q (1–5), ky=0.45	55
12	STD2	ky scan (0.10→ 2.0) @ q=2,4 w/ a/L_T=6	32
13	STD2	ky scan (2.0→ 24.0) @ q=2,4 w/ a/L_T=6	32

* STD = 398 GKS runs, STD2 = 310 GKS runs

STD case: $R/a=3.0$, $r/a=0.5$, $q=2.0$, $s=1.0$, $\alpha=0$, $a/L_T=3.0$, $a/L_n=1.0$, $T_i/T_e=1.0$, $\nu=0$, $\beta=0$
TEM1 Case: STD w/ $a/L_n=2$, $a/L_T=2$ TEM2 Case: STD w/ $a/L_n=3$, $a/L_T=1$
PED case: $R/a=3.0$, $r/a=0.75$, $q=4.0$, $s=3.0$, $\alpha=5$, $a/L_T=10.0$, $a/L_n=3.0$, $T_i/T_e=1.0$, $\nu=0$, $\beta=0$

Linear GKS Database for NCS, PED Cases

Scan	Set	Scan type	# pts
14	NCS	ky scan (0.01→0.70) @ various q (1→5)	80
15	NCS	shear scan (-1→2) @ various q(1→5)	55
16	NCS	shear scan (-1→2) @ various q(1→5), α=1	55
17	NCS	shear scan (-1→2) @ various q(1→5), α=2	55
18	NCS	shear scan (-1→2) @ various q(1→5), α=3	55
19	NCS	shear scan (-1→2) @ various q(1→5), α=4	55
20	NCS	ky scan (0.01→0.70) @ various a/L_T (2→5)	64
21	NCS	ky scan (0.01→0.70) @ various T_i/T_e (0.5→2.0)	64
22	PED	ky scan (0.01→0.70) @ various q (3→7)	80
23	PED	shear scan (1→7) @ various q (3→7), α=0	80
24	PED	shear scan (1→7) @ various q (3→7), α=3	80
25	PED	shear scan (1→7) @ various q (3→7), α=6	80
26	PED	shear scan (1→7) @ various q (3→7), α=9	80
27	PED	shear scan (1→7) @ various q (3→7), α=12	80
28	PED	ky scan (0.01→0.70) @ various a/L_T (7→12), α=0	64
29	PED	ky scan (0.01→0.70) @ various T_i/T_e (0.5→2.0)	64

* NCS = 483 GKS runs, PED = 608 GKS runs

Transport Database for TGLF Testing

Scan	Set	Scan type	# pts
1	STD	Magnetic shear scan @ MHD alpha=0, 1, 2	20
2	STD	Magnetic shear scan @ a/Ln=0.5, 1.5	12
3	STD	Magnetic shear scan @ q=1.25	7
4	STD	Safety factor scan @ s=1.0	7
5	STD	a/L_T scan @ a/L_n=0.5, 1.0, 1.5	27
6	STD	T_i / T_e scan (0.5, 1.0, 1.5, 2.0)	4
7	STD	r/a scan (0.10, 0.25, 0.50, 0.75, 1.0)	5
8	STD	R/a scan (1.75, 2.0, 2.5, 3.0, 3.5, 4.0, 5.0)	7
9	TEM1	Safety factor scan (q=1.1, 1.25, 2.0, 2.5, 3.0, 4.0)	6
10	TEM1	Magnetic shear scan @ q=2	4
10	TEM2	Safety factor scan (q=1.1, 1.5, 2.0, 2.5, 3.0, 4.0)	6
11	STD	a/L_n scan @ a/L_T=2.0, 3.0	7
12	STD	a/L_T scan @ r/a=0.75	6
13	PED	Magnetic shear scan (s=1.0, 1.5, 2.0, 2.5, 3.0)	5
14	PED	a/L_T scan	4
15	STD	Safety factor scan @ s=-0.5, 1.0, 1.5	20
16	TEM2	Safety factor scan @ s=1.0	6
17	TEM1	Magnetic shear scan @ q=2	7
18	TEM2	Magnetic shear scan @ q=2	8
19	STD	Collisionality scan (ν_{ei}=0.0 – 0.5)	8
20	STD	ExB shear scan (γ_E=0.0 – 0.4, γ_p=0)	5
21	STD	Elongation scan scan w/ Miller geometry, κ=1.0 (κ=1.0–2.5)	7
22	STD	Triangularity scan w/ Miller geometry, κ=1.0 (δ=0.0–0.75)	4
23	STD	Aspect ratio (R/a) scan w/ κ=1.0 (A=1.2–4.0)	5

Database used in fitting (scans 1–14)

STD case: R/a=3.0, r/a=0.5, q=2.0, s=1.0, α=0, a/L_T=3.0, a/L_n=1.0, T_i/T_e=1.0, ν=0, β=0
TEM1 Case: STD w/ a/L_n=2, a/L_T=2   TEM2 Case: STD w/ a/L_n=3, a/L_T=1
PED case: R/a=3.0, r/a=0.75, q=4.0, s=3.0, α=5, a/L_T=10.0, a/L_n=3.0, T_i/T_e=1.0, ν=0, β=0

Experimental Data and Theory Issues Need Addressing in Order to Move Transport Simulations beyond ρ=0.84

- **RMS errors increase noticably for DIII-D and TFTR L-modes when ρ_{BC} changed from 0.84 to 0.90**
- **Experimental analysis issues**
  - Sharp changes in q-profiles near edge, non monotonic magnetic shear
  - More accurate equilibrium (e.g. EFITs) needed
  - Better Zeff measurements which impacts ion density profile
  - Toroidal rotation profile, held fixed in these simulations
- **Theory/modeling issues**
  - ExB shear quench rule needs further examination (GYRO shows elongation dependence)
  - More ETG simulations needed for near edge conditions
  - Low a/Lt, TEM regime needs further study
  - More comparisons between TGLF and GYRO for edge conditions